Diffusion MRI of brain pathways

UCLA LINT NITP
7.12.2013

Van J Wedeen, MD
Department of Radiology, Massachusetts General Hospital
AA Martinos Center for Biomedical Imaging
van@nmr.mgh.harvard.edu

Crick & Jones, Nature, 1993 -

“It is intolerable that we do not have a knowledge of the connectivity of the human brain”

Jeff Lichtman, Science, 2011 -

"The relation between the structure of the nervous system and its function is more poorly understood ... than any other organ system.”

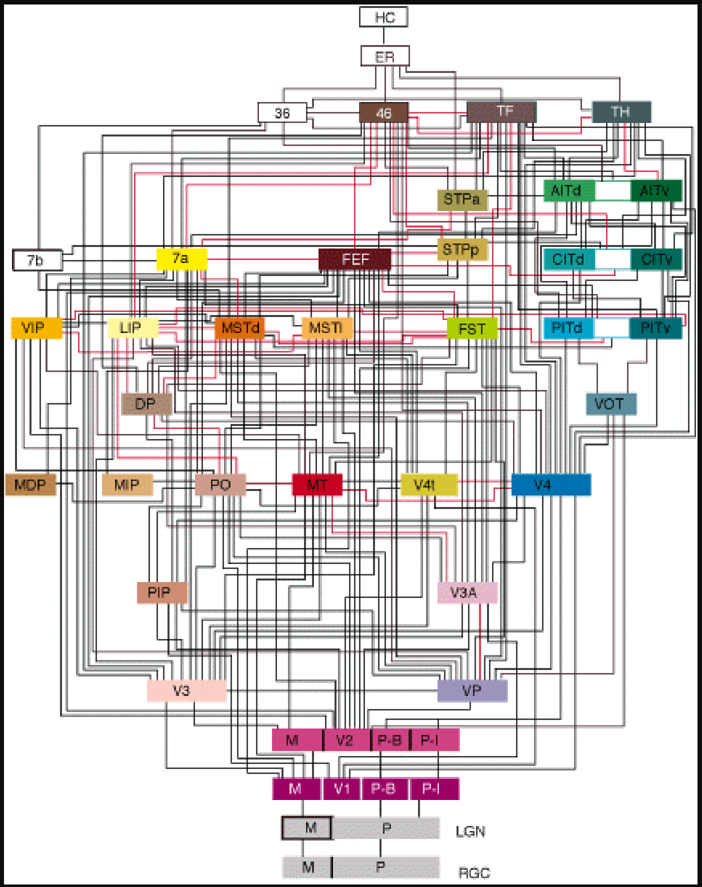

Felleman & Van Essen, rhesus visual system Science 1989

OHBM Paris 1995
dMRI tractography proposed and DTI in two forms, and noted unable to resolve crossing

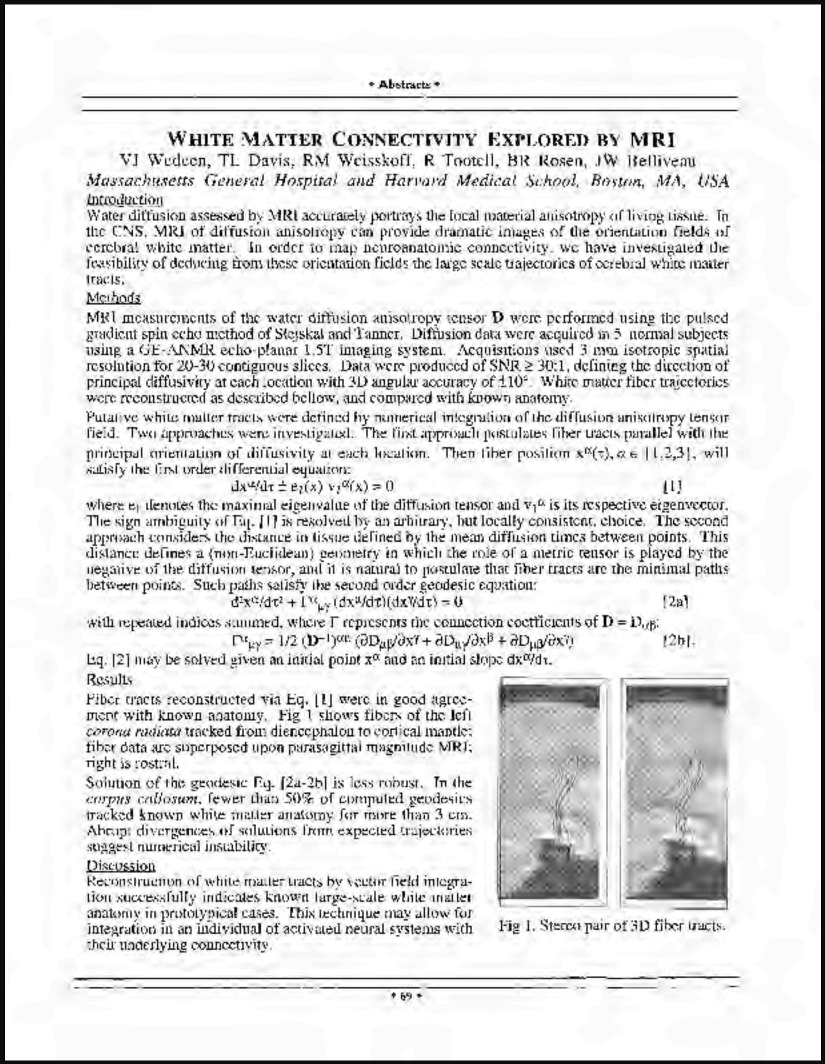

WHITE MATTER CONNECTIVITY EXPLORED BY MRI

VJ Wedeen, TL Davis, RM Weisskoff, R Tootell, BR Rosen, JW Belliveau
Massachusetts General Hospital and Harvard Medical School, Boston, MA, USA

Introduction

Water diffusion assessed by MRI accurately portrays the local material anisotropy of living tissue. In the CNS, MRI of diffusion anisotropy can provide dramatic images of the orientation fields of cerebral white matter. In order to map neuroanatomic connectivity, we have investigated the feasibility of deducing from these orientation fields the large scale trajectories of cerebral white matter tracts.

Methods

MRI measurements of the water diffusion anisotropy tensor **D** were performed using the pulsed gradient spin echo method of Stejskal and Tanner. Diffusion data were acquired in 5 normal subjects using a GE-ANMR echo-planar 1.5T imaging system. Acquisitions used 3 mm isotropic spatial resolution for 20-30 contiguous slices. Data were produced of SNR ≥ 30:1, defining the direction of principal diffusivity at each location with 3D angular accuracy of ±10°. White matter fiber trajectories were reconstructed as described bellow, and compared with known anatomy.

Putative white matter tracts were defined by numerical integration of the diffusion anisotropy tensor field. Two approaches were investigated. The first approach postulates fiber tracts parallel with the principal orientation of diffusivity at each location. Then fiber position $x^\alpha(\tau), \alpha \in \{1,2,3\}$, will satisfy the first order differential equation:

$$dx^\alpha/d\tau \pm e_1(x)\, v_1^\alpha(x) = 0 \qquad [1]$$

where e_1 denotes the maximal eigenvalue of the diffusion tensor and v_1^α is its respective eigenvector. The sign ambiguity of Eq. [1] is resolved by an arbitrary, but locally consistent, choice. The second approach considers the distance in tissue defined by the mean diffusion times between points. This distance defines a (non-Euclidean) geometry in which the role of a metric tensor is played by the negative of the diffusion tensor, and it is natural to postulate that fiber tracts are the minimal paths between points. Such paths satisfy the second order geodesic equation:

$$d^2x^\alpha/d\tau^2 + \Gamma^\alpha_{\beta\gamma}\,(dx^\beta/d\tau)(dx^\gamma/d\tau) = 0 \qquad [2a]$$

with repeated indices summed, where Γ represents the connection coefficients of $\mathbf{D} = D_{\alpha\beta}$:

$$\Gamma^\alpha_{\beta\gamma} = 1/2\,(\mathbf{D}^{-1})^{\alpha\mu}\,(\partial D_{\mu\beta}/\partial x^\gamma + \partial D_{\mu\gamma}/\partial x^\beta + \partial D_{\mu\beta}/\partial x^\gamma) \qquad [2b].$$

Eq. [2] may be solved given an initial point x^α and an initial slope $dx^\alpha/d\tau$.

Results

Fiber tracts reconstructed via Eq. [1] were in good agreement with known anatomy. Fig 1 shows fibers of the left *corona radiata* tracked from diencephalon to cortical mantle; fiber data are superposed upon parasagittal magnitude MRI; right is rostral.

Solution of the geodesic Eq. [2a-2b] is less robust. In the *corpus callosum*, fewer than 50% of computed geodesics tracked known white matter anatomy for more than 3 cm. Abrupt divergences of solutions from expected trajectories suggest numerical instability.

Discussion

Reconstruction of white matter tracts by vector field integration successfully indicates known large-scale white matter anatomy in prototypical cases. This technique may allow for integration in an individual of activated neural systems with their underlying connectivity.

Fig 1. Stereo pair of 3D fiber tracts.

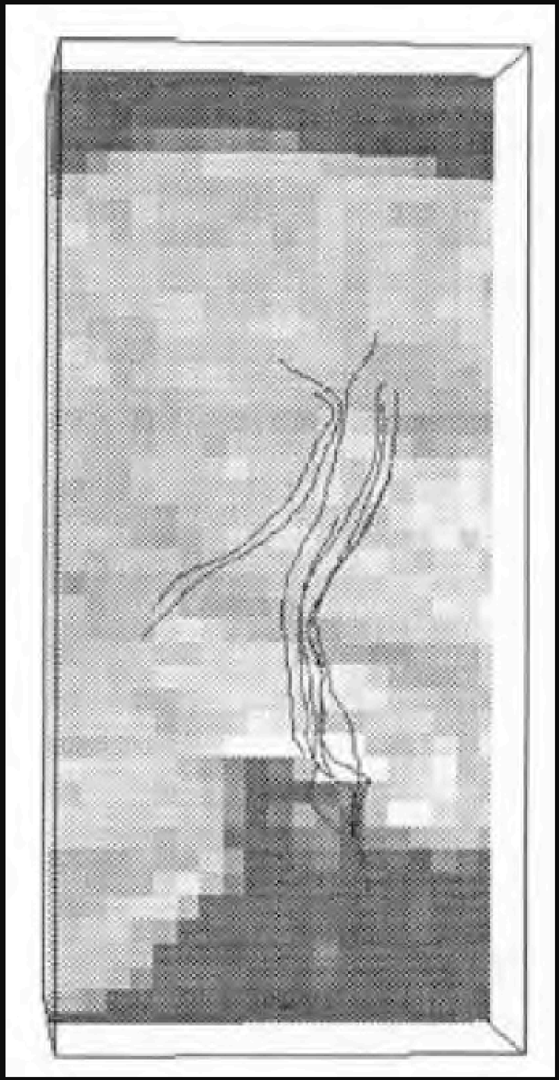

Wedeen et al HBP Paris 1995

Blood flow - 1985

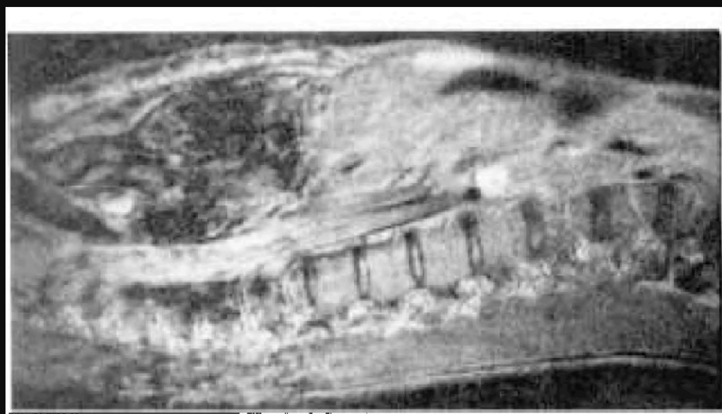

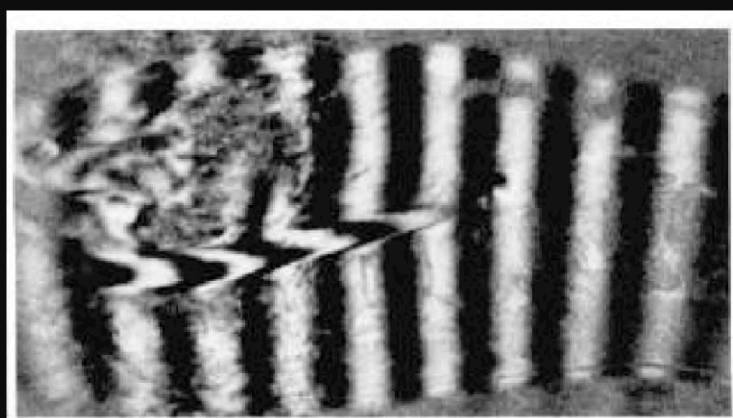

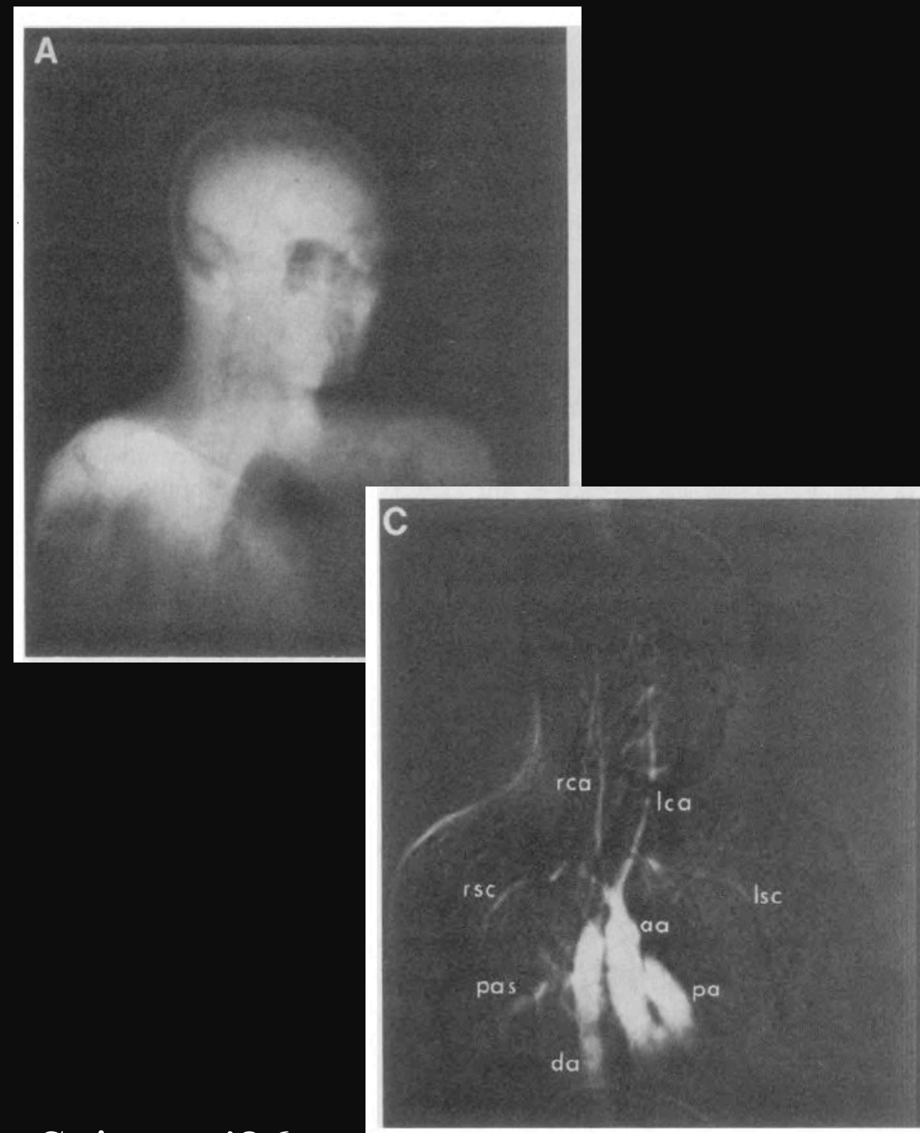

MR angio Science '86

MRI tractography reveals the functional architecture of the heart

equal fiber shortening across the wall; a compliant slip system; 2x dynamic regime; design saturation

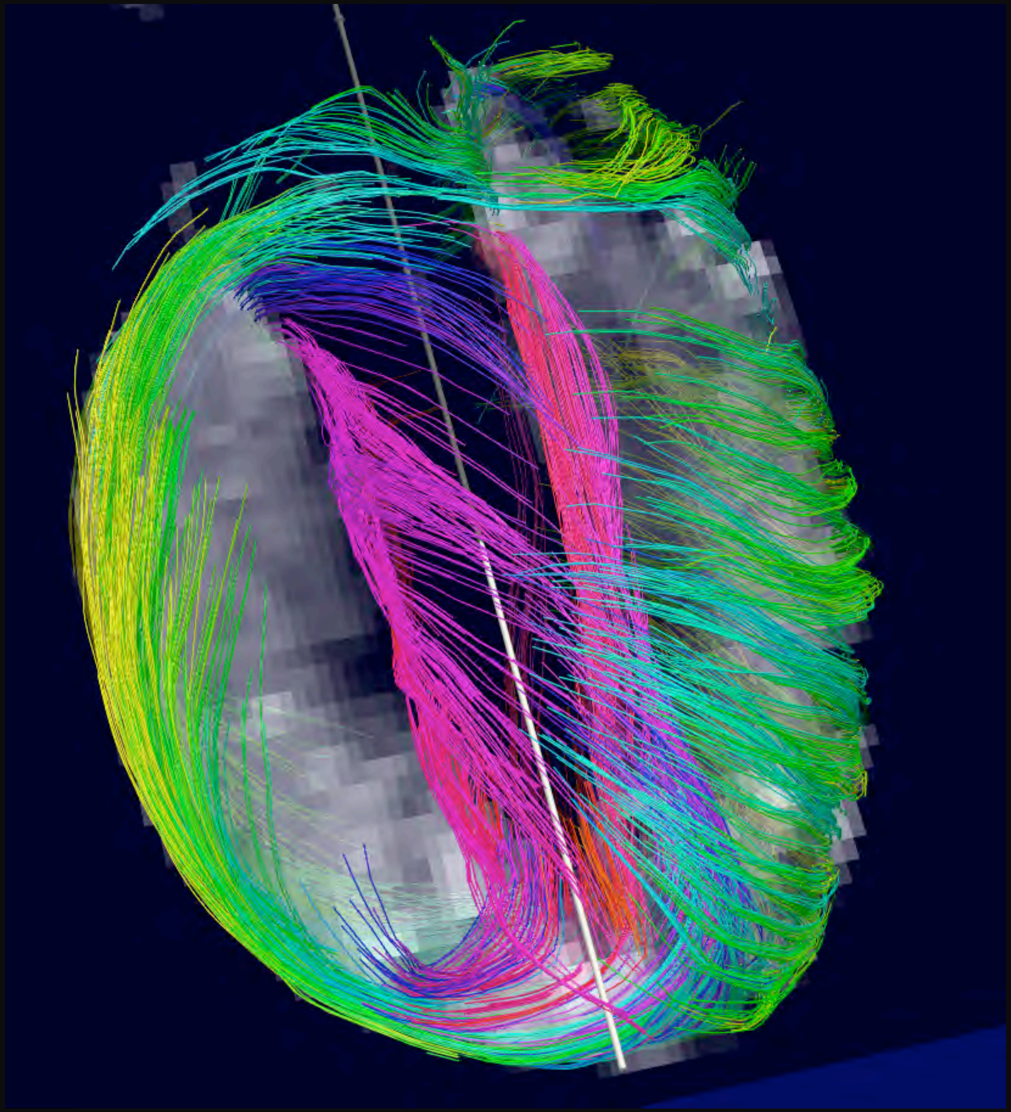

Sosnovick et al,

Pathway overlap is a defining characteristic of the brain

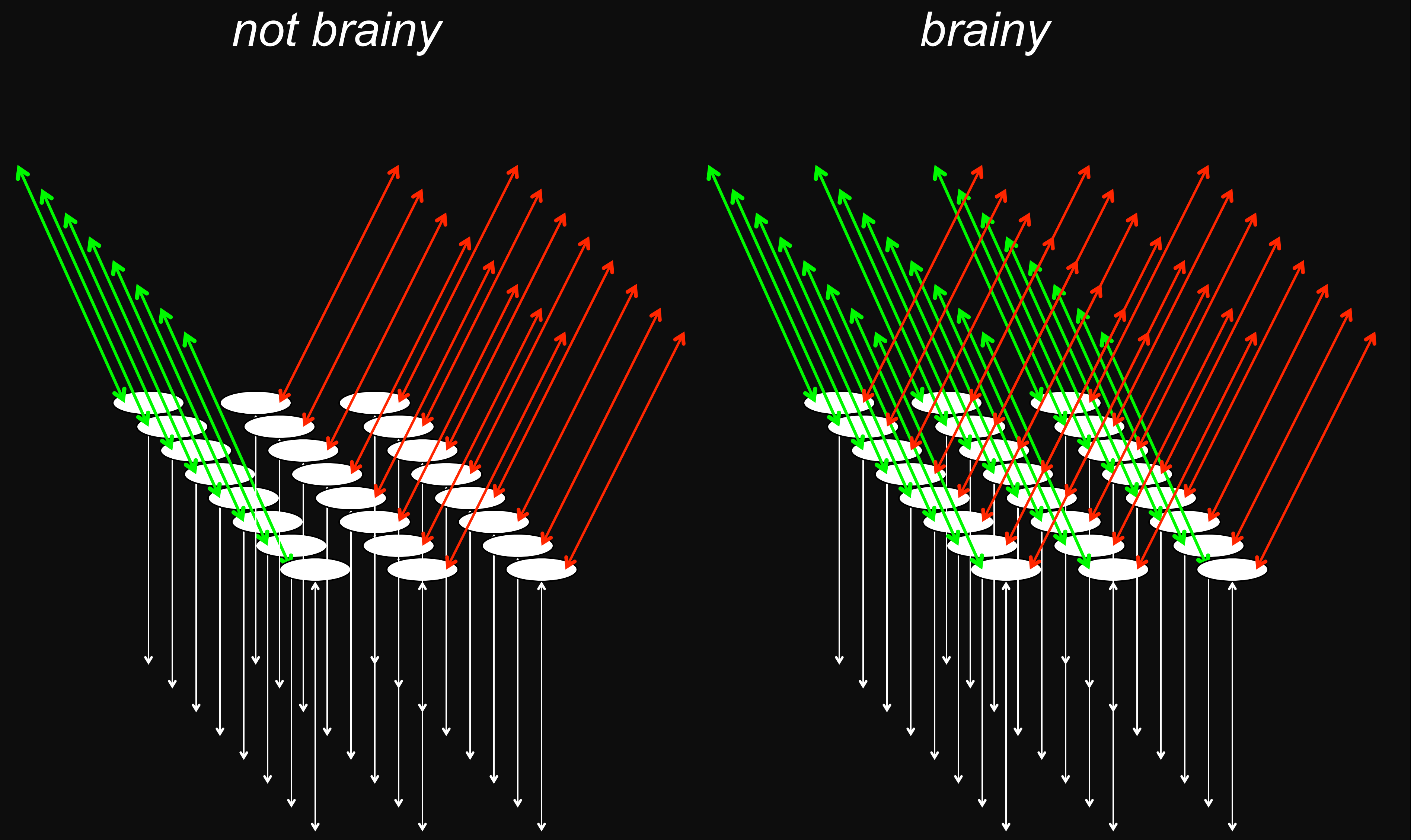

Neuroanatomy is more difficult than other anatomy because many structures can overlap in the same place

macaque tracers - Pandya & Schmahmann

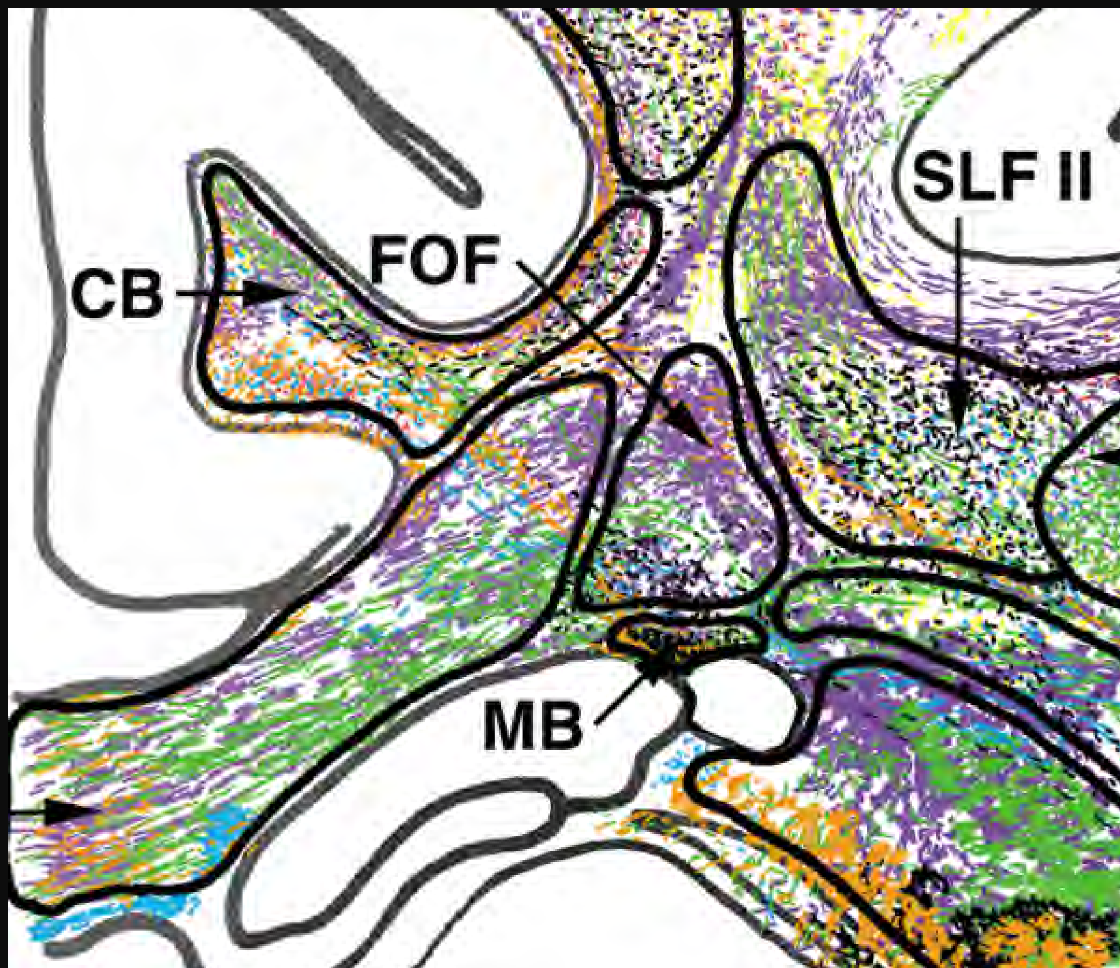

2D x-ray, overlap

3D CT, no overlap

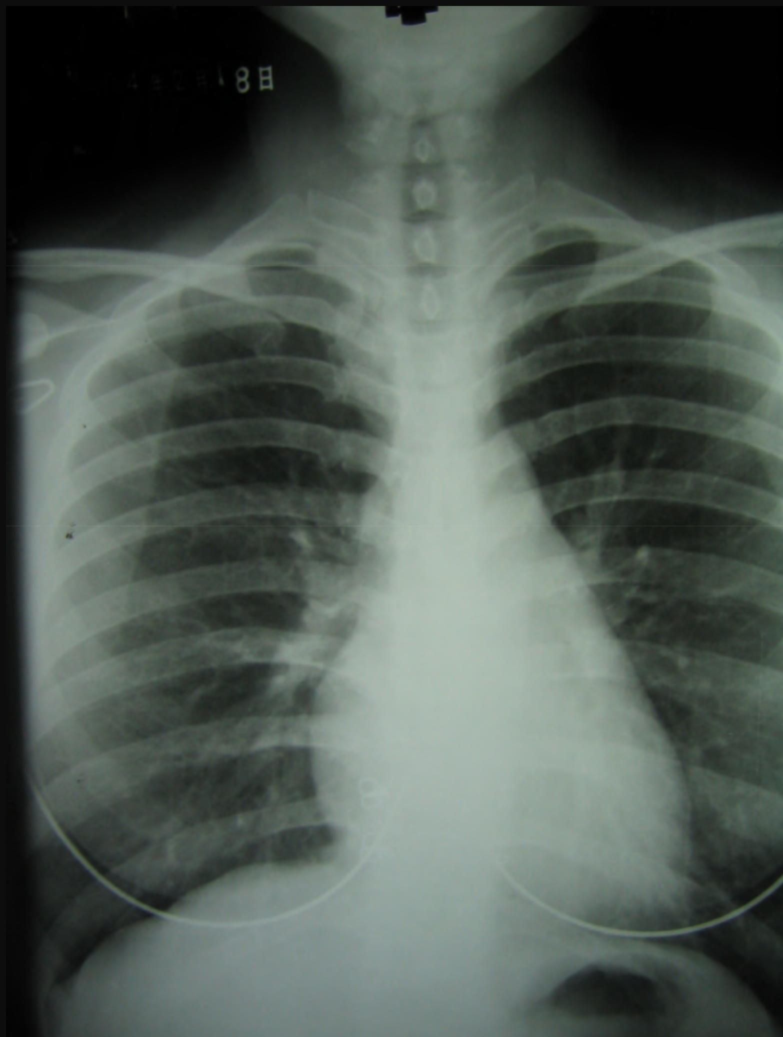

Diffusion MRI -

3D pattern of water diffusion indicates tissue structure

1994: diffusion tensors show average fiber directions

tissue

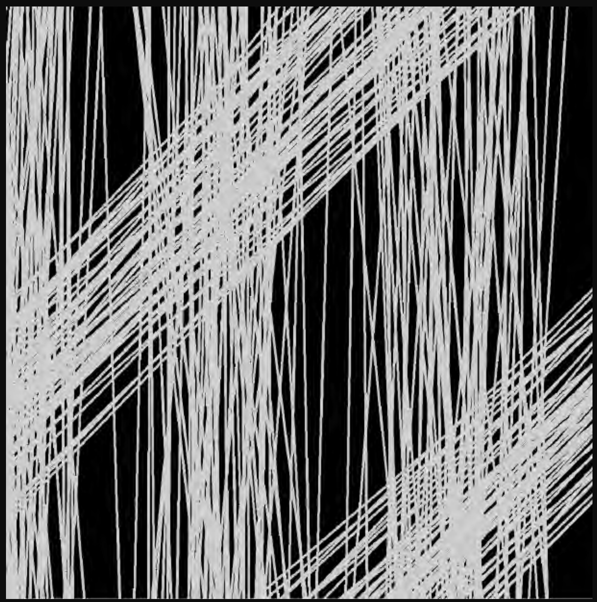

diffusion tensor

Water diffusion traces tissue fiber structure

diffusion spectrum MRI (DSI) resolves overlapping pathways

brain tissue

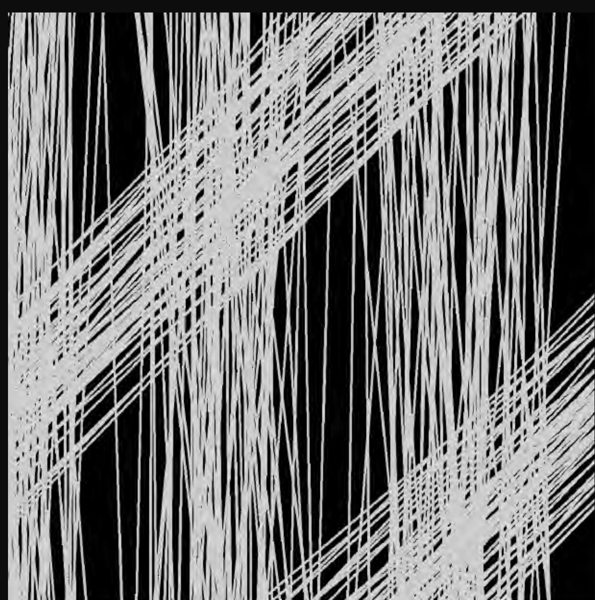

“image” of diffusion

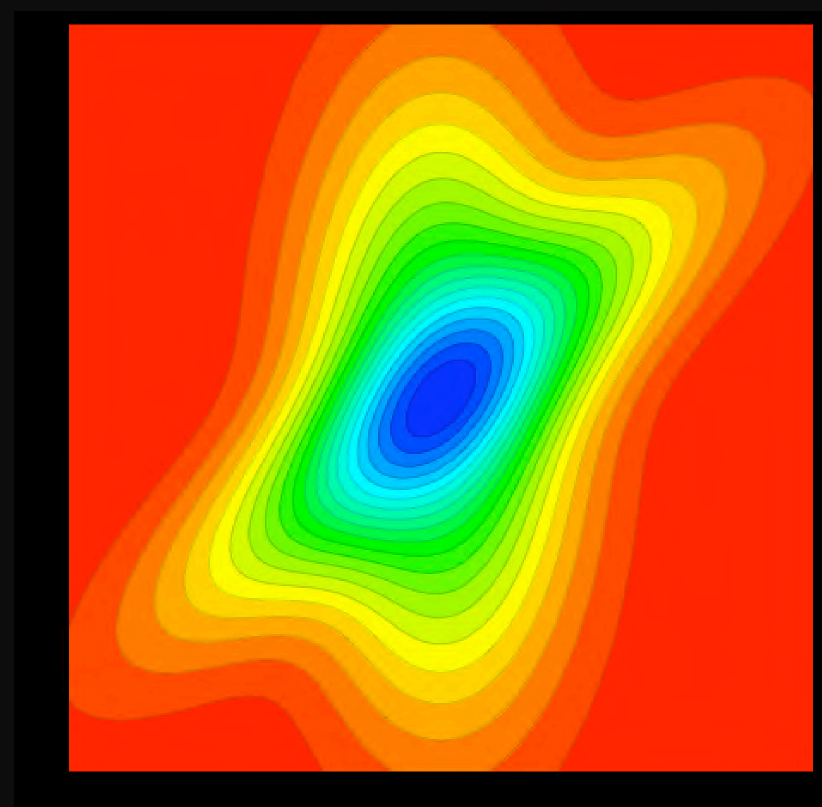

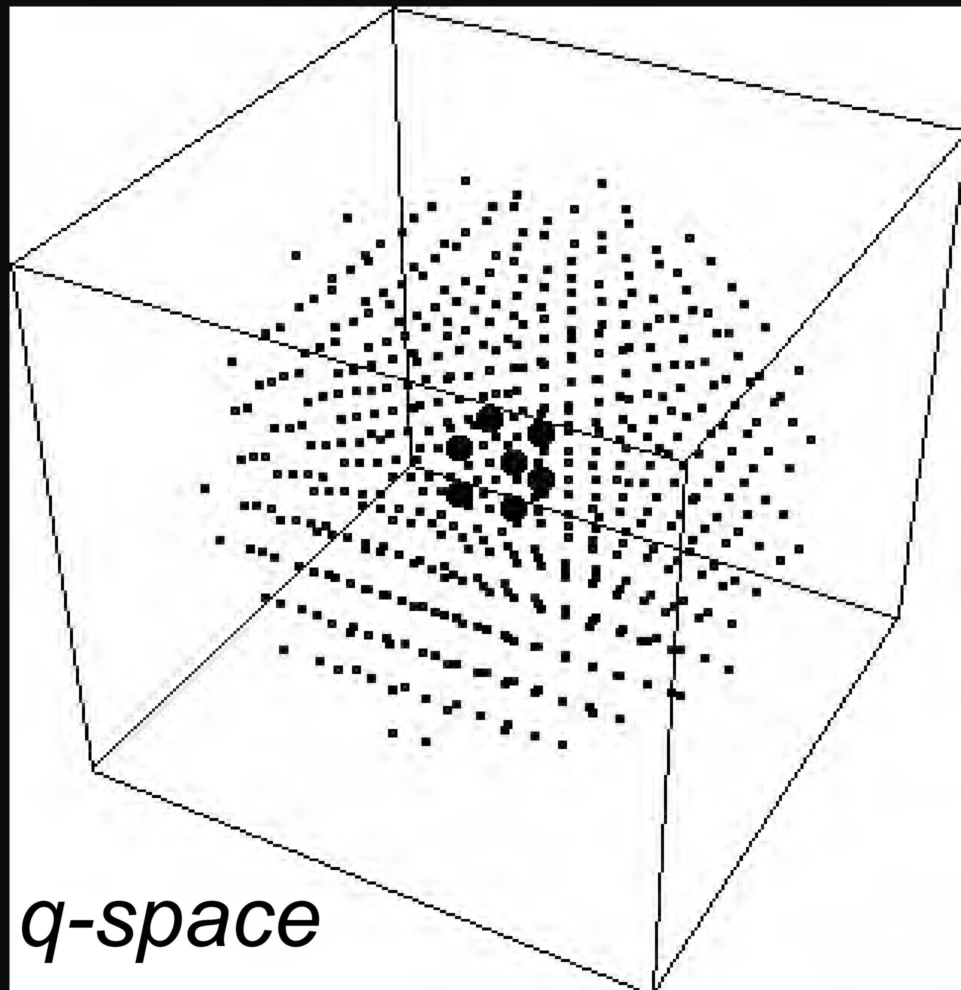

DTI: 7 q-samples, recon with tensor fit
DSI: 500 q-samles, recon with 3DFT

DSI encoding and reconstruction

q samples

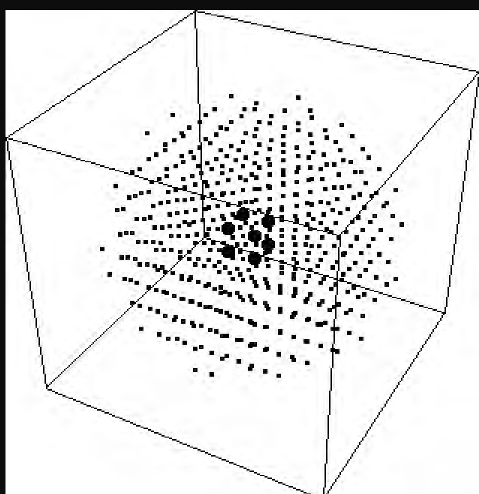

FT ➔

pdf level set

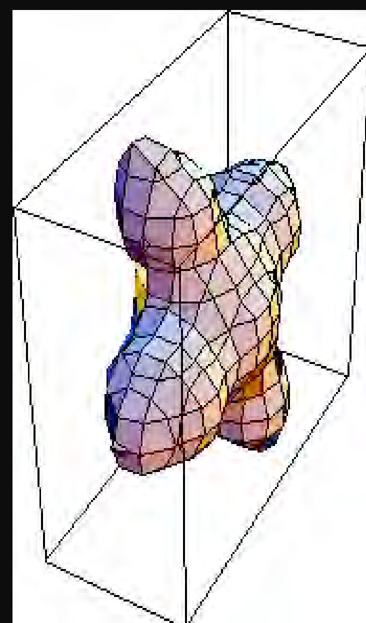

∫dr ➔

odf spherical plot

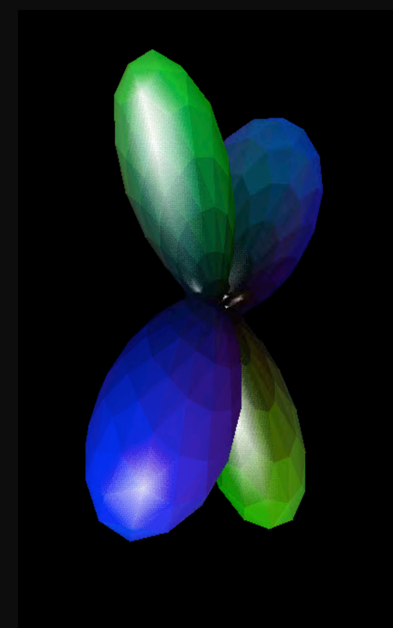

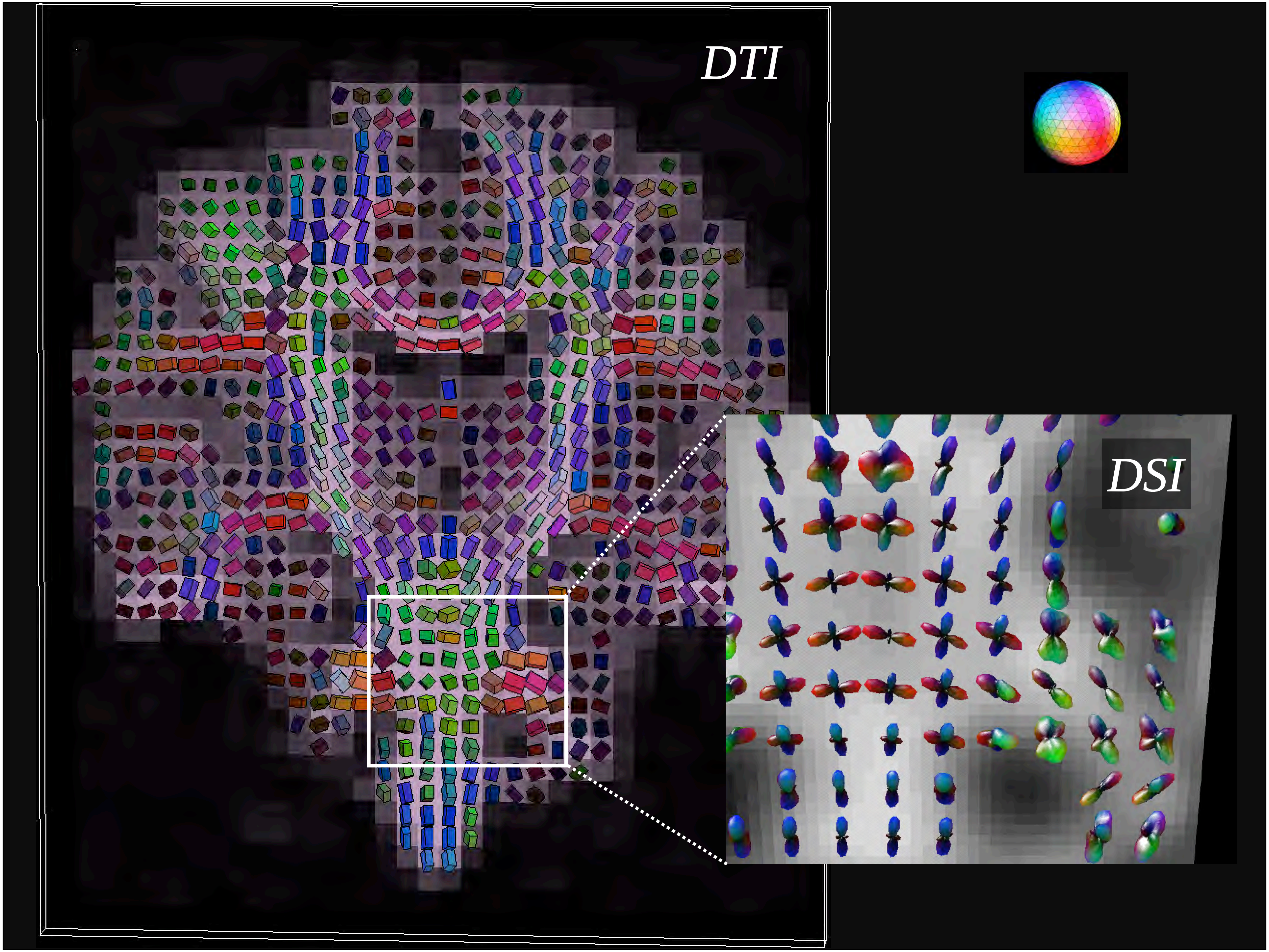
DTI
DSI

DSI directions of maximum diffusion 3T human in vivo

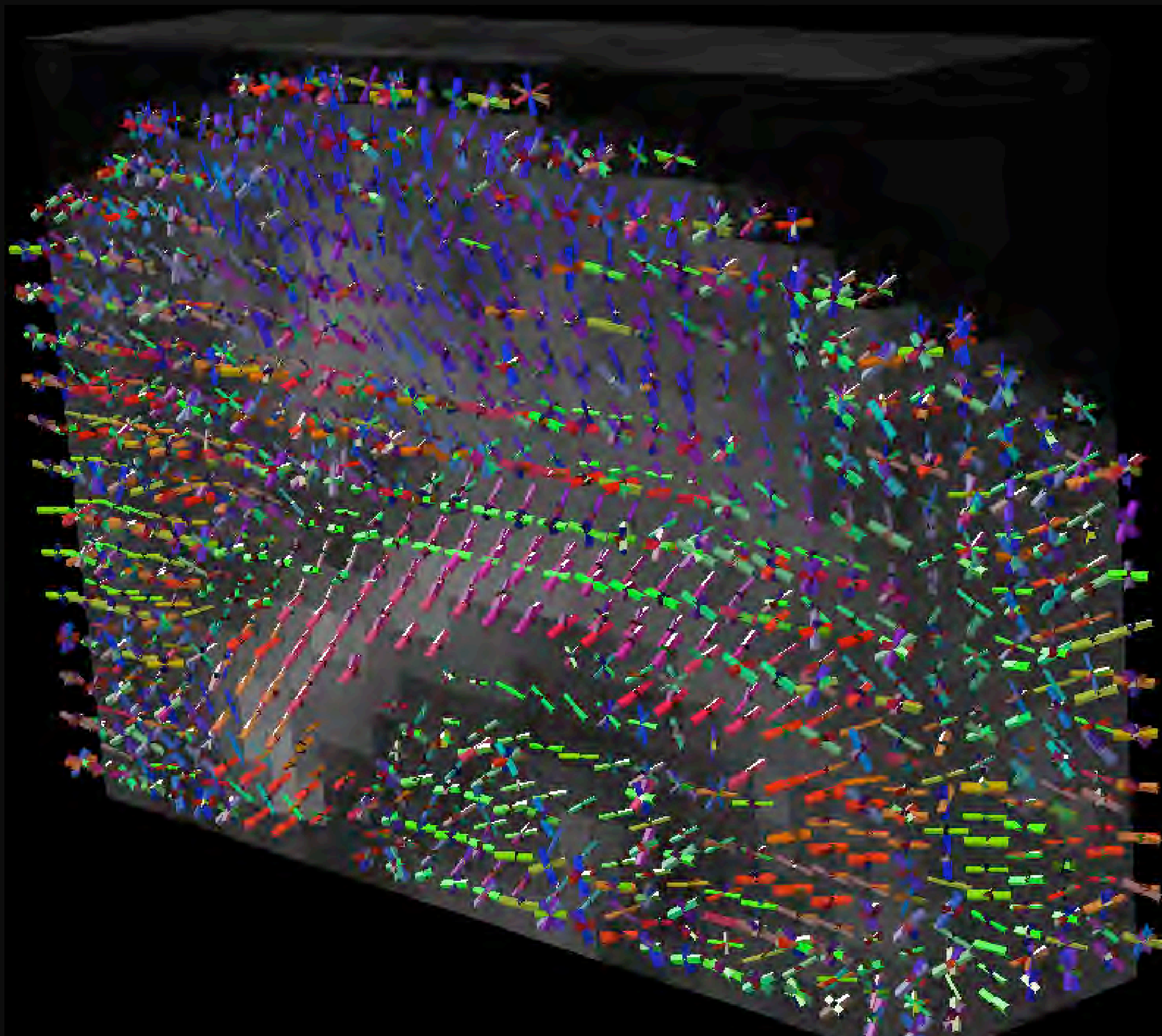

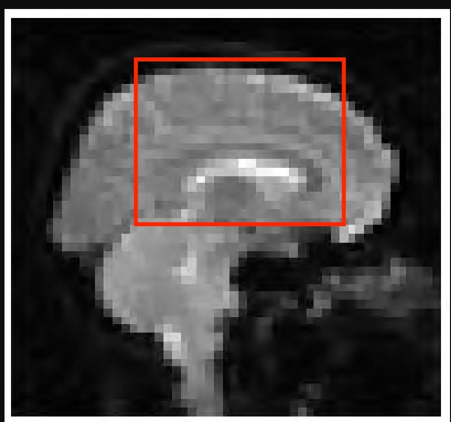

To de-singularize the brain, resolve fiber orientations at each location - with DSI

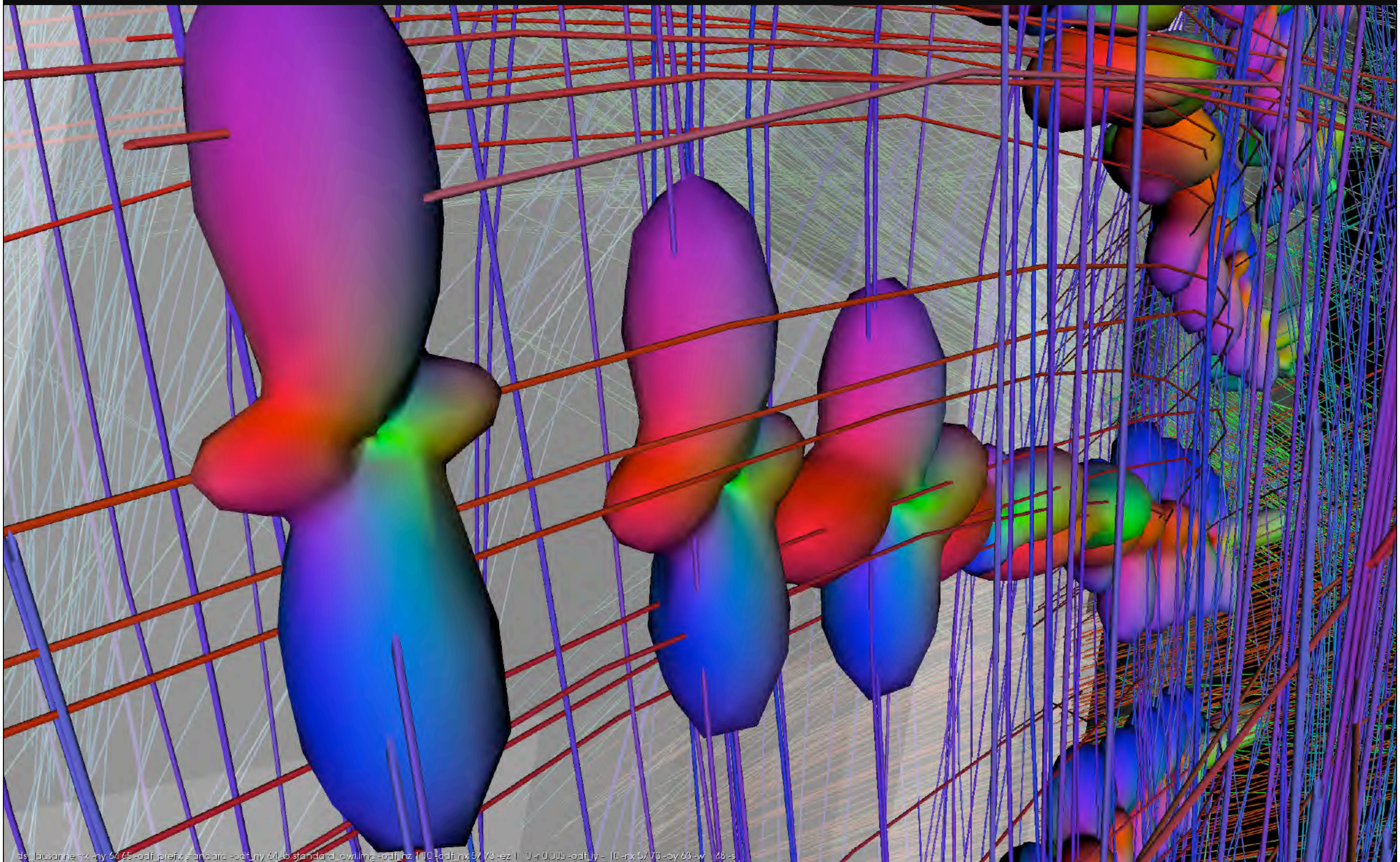

DSI tractography - Pons normal human subject in vivo
middle cerebellar peduncle - red
corticospinal tract - blue

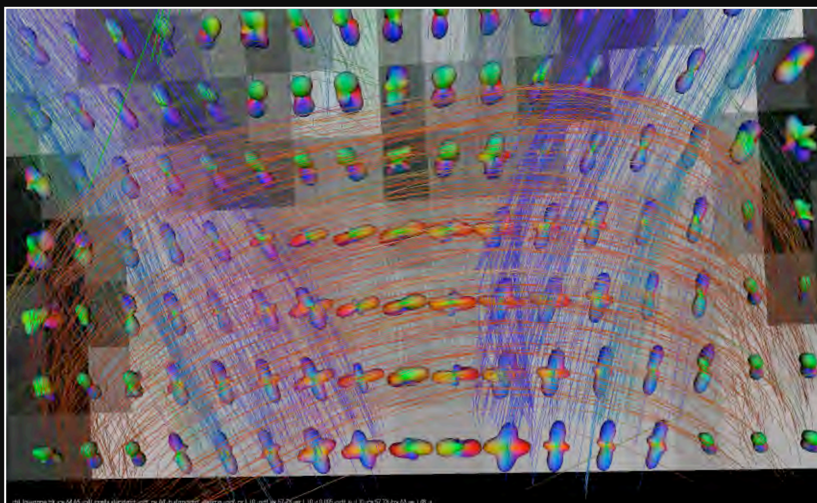

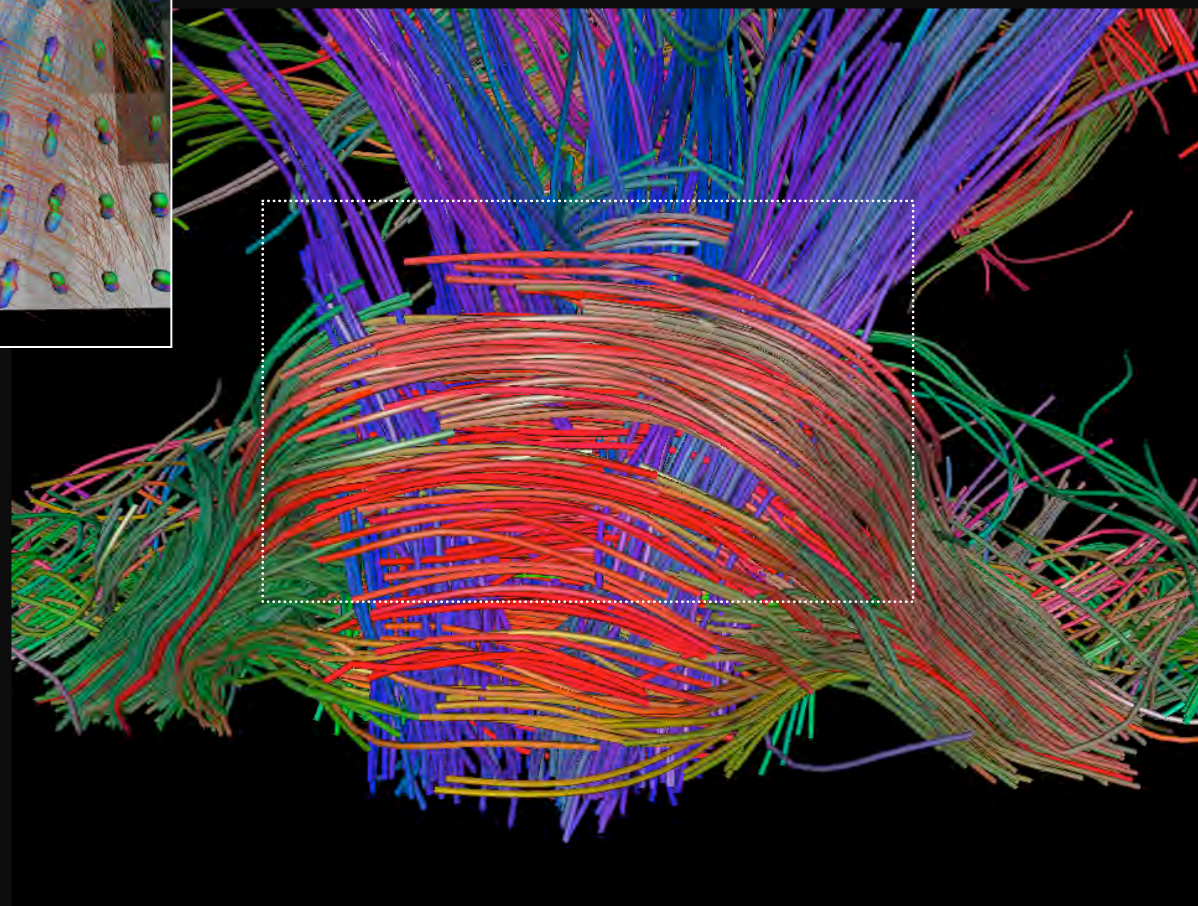

3T DSI SE 3500/96
2.6mm b_{max}8500 53min

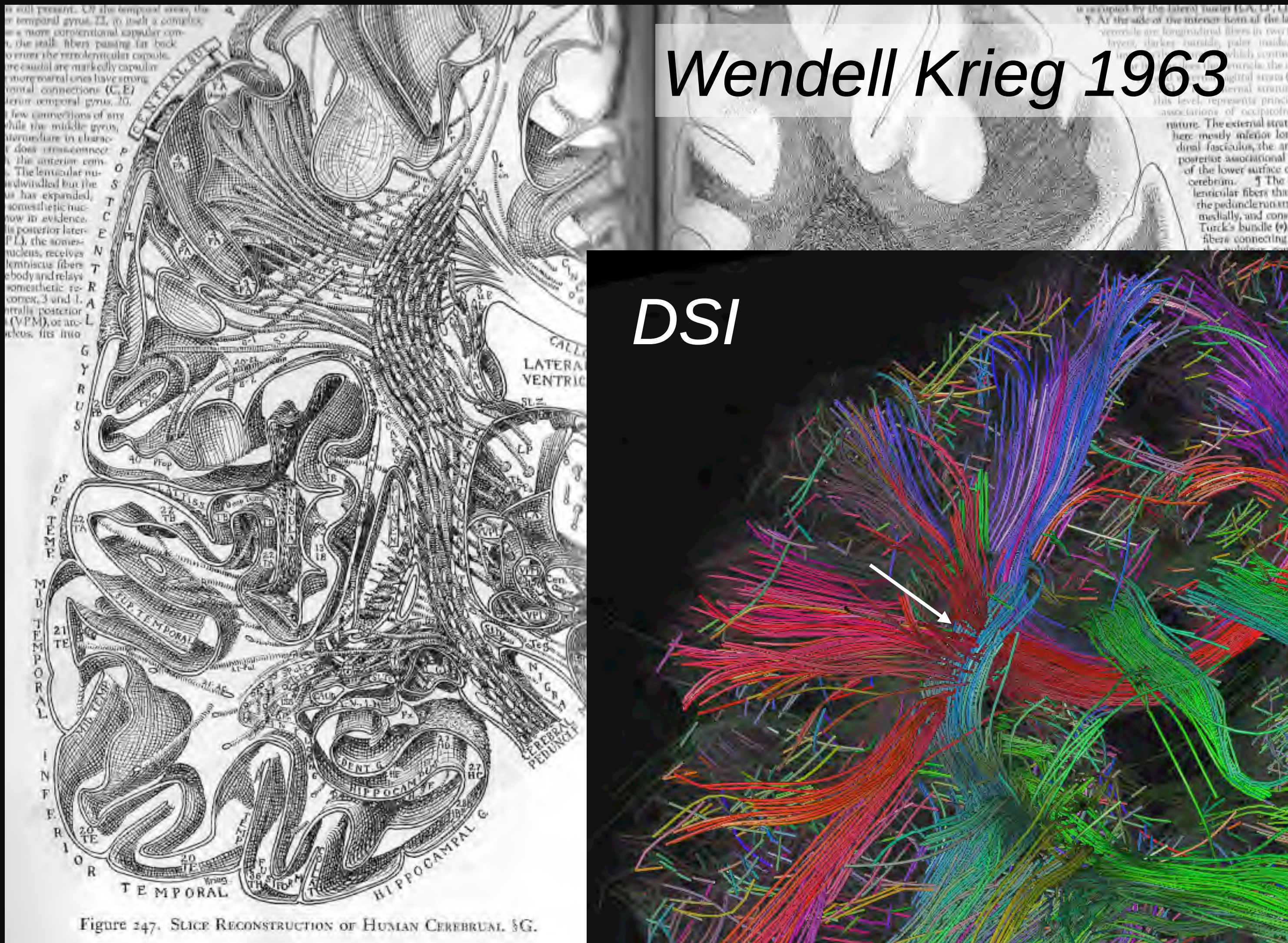

Figure 247. Slice Reconstruction of Human Cerebrual. §G.

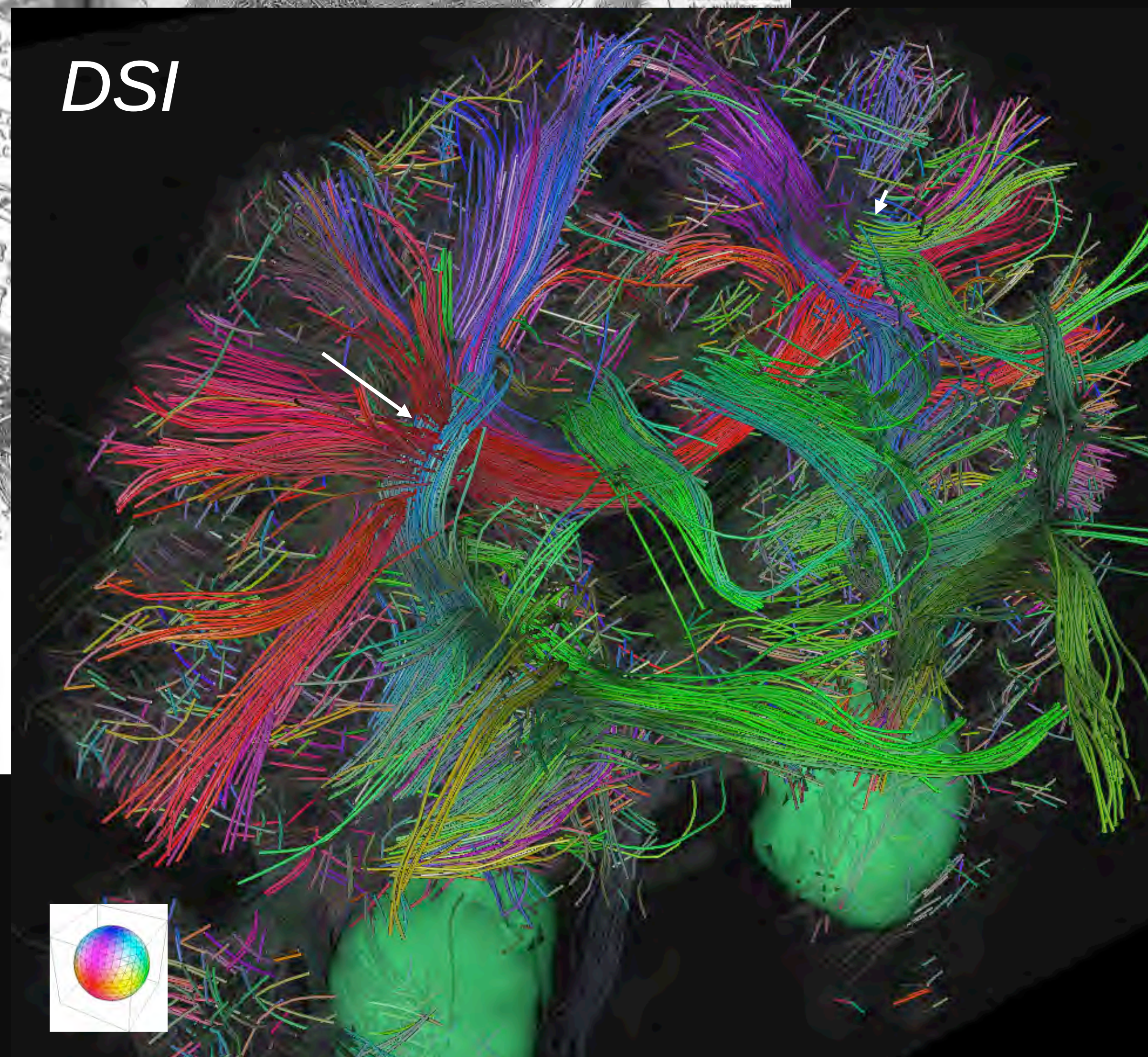

3T 2.6mm 8500 b_{max}

Human DSI

whole brain

sagittal slice

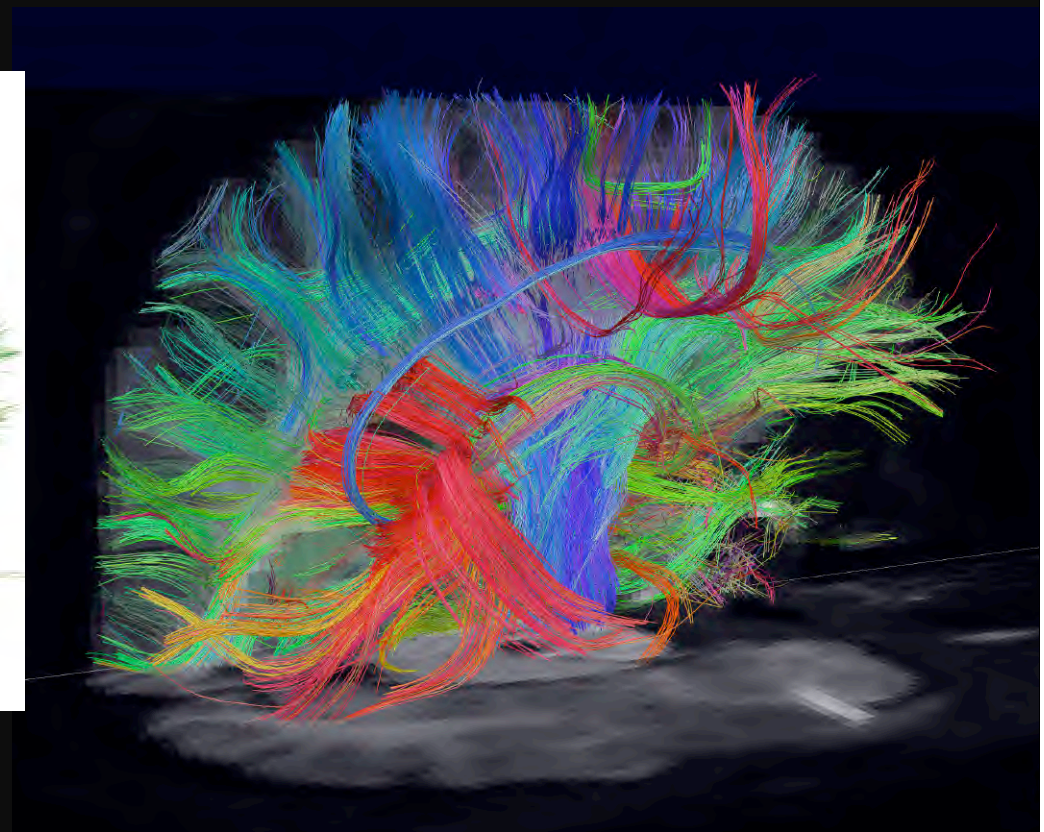

DSI rhesus hemisphere

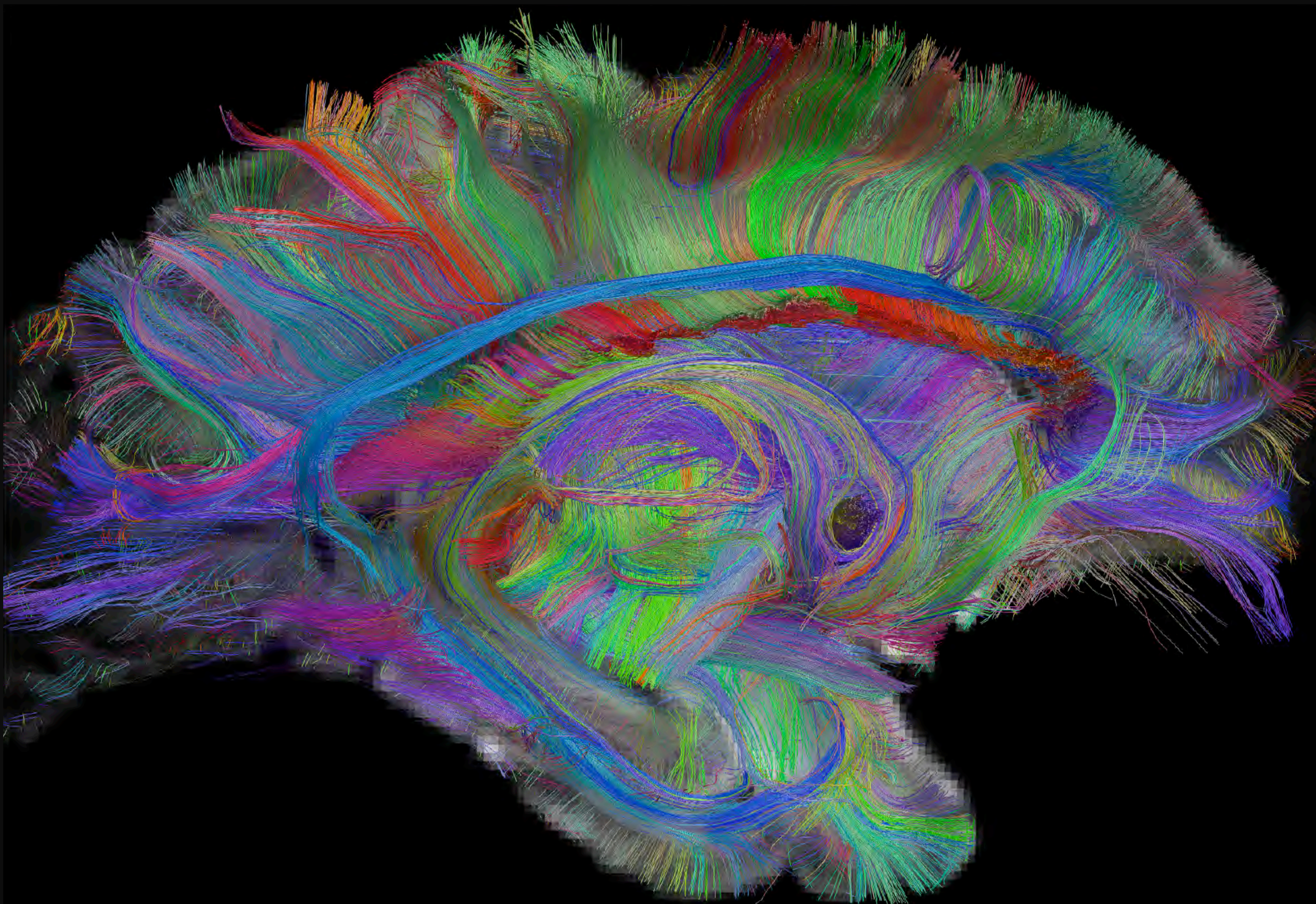

Owl monkey

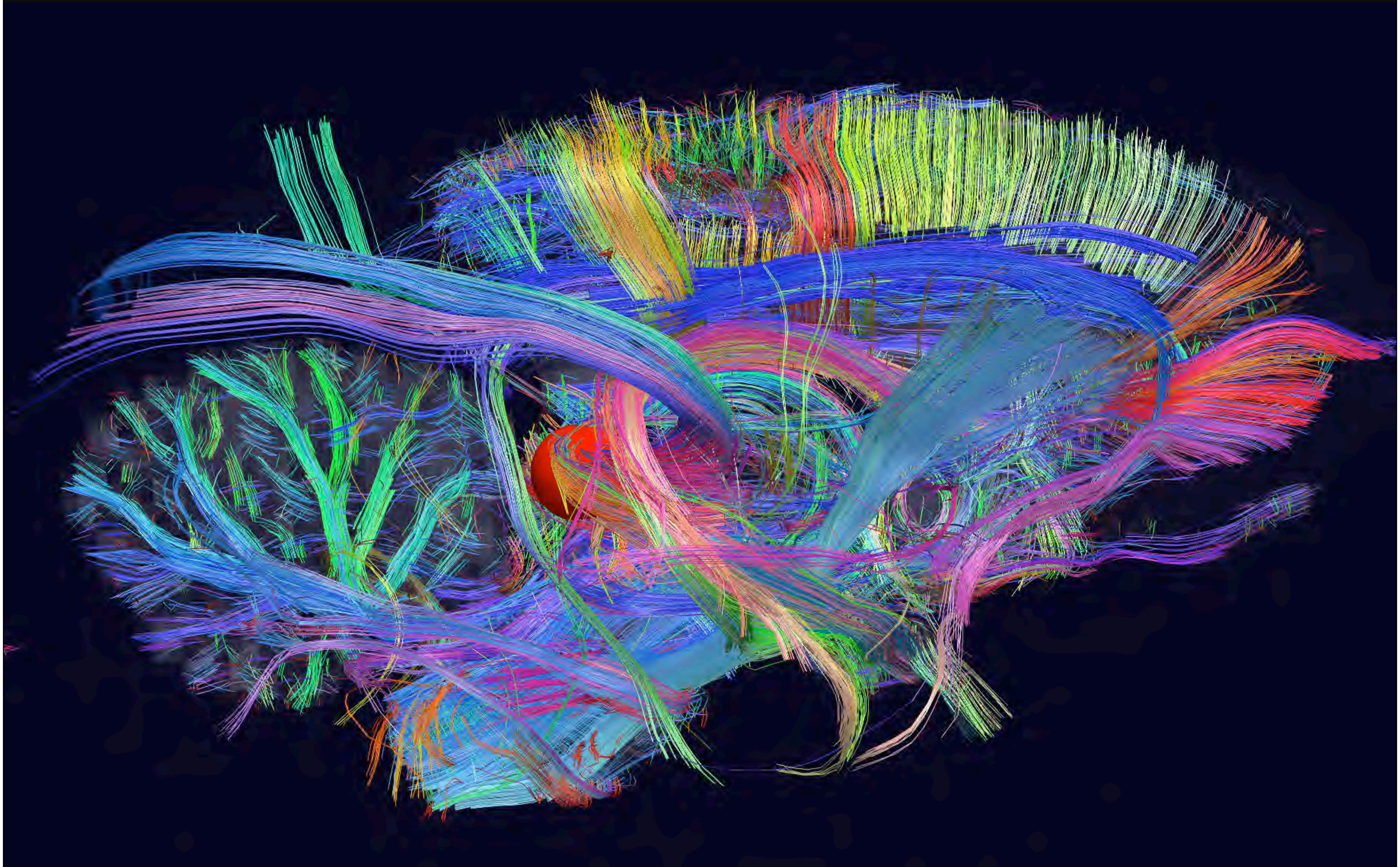

Animal models - DSI neurorat

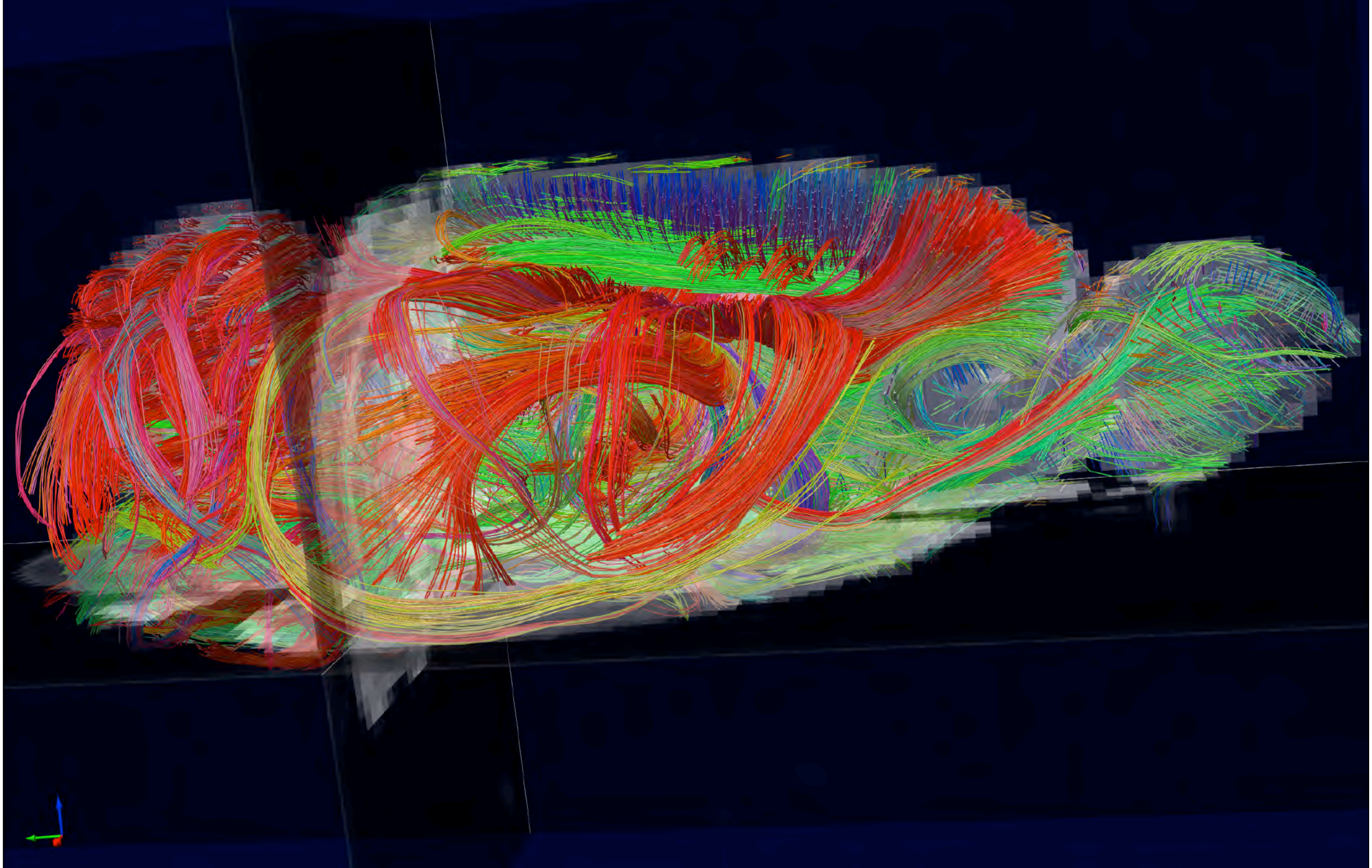

Optic chiasm

Figure 3.6. The Functional Anatomy of the Optic Nerves, Chiasm and Tracts to the Geniculate Body

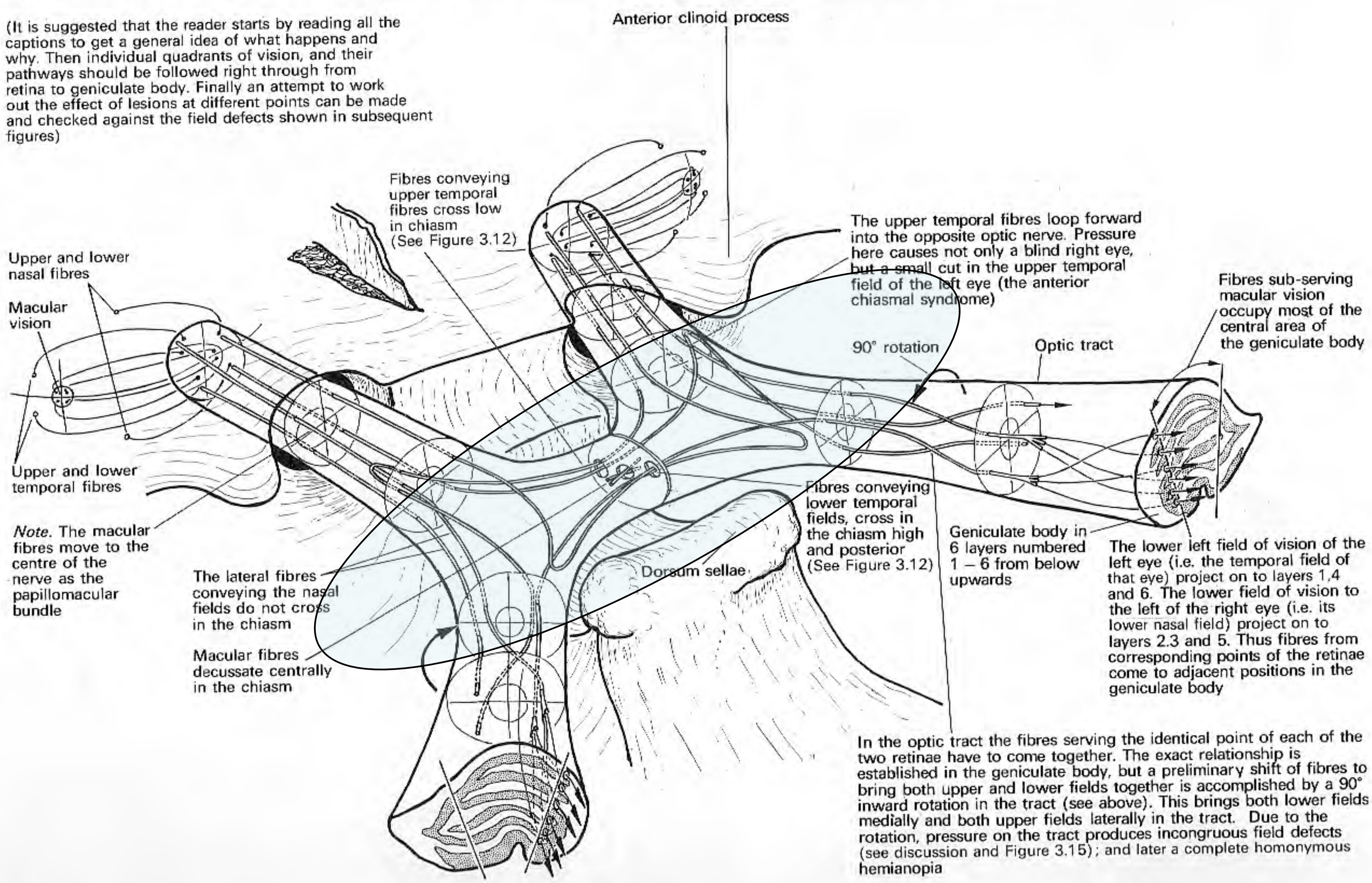

Optic chiasm

DSI

DTI

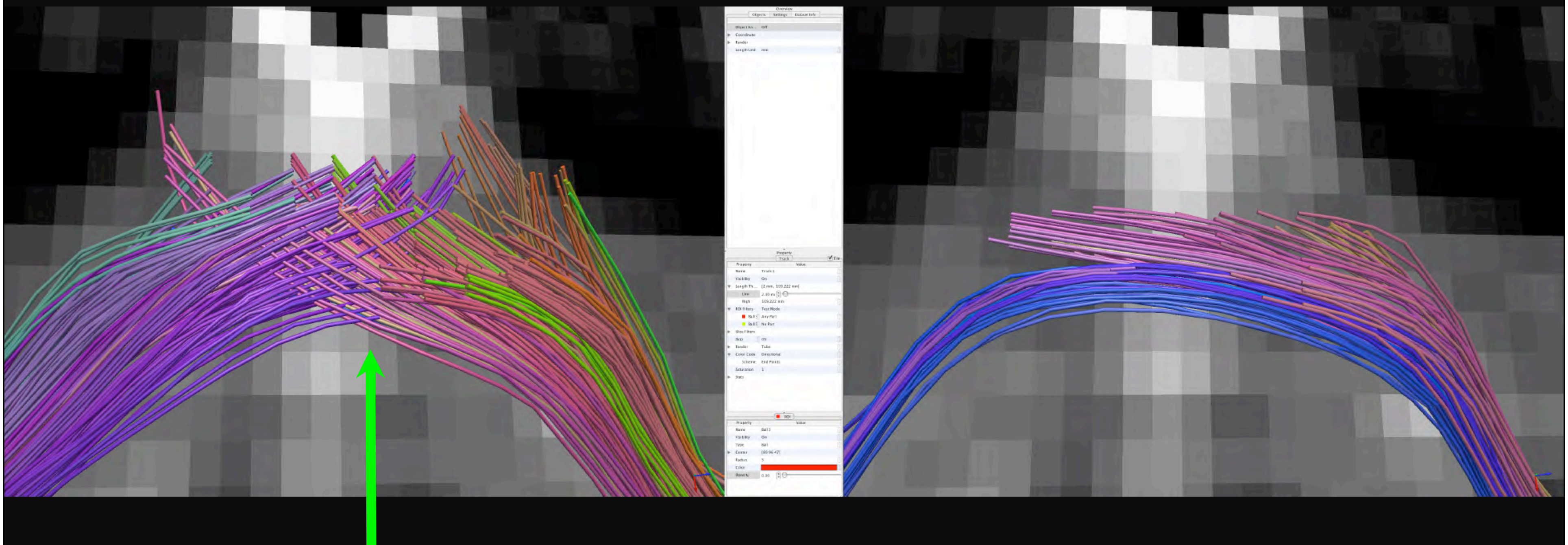

descussation

Wedeen et al Neruoimage 2008 in press

Macaque centrum semiovale

tracer - 3D

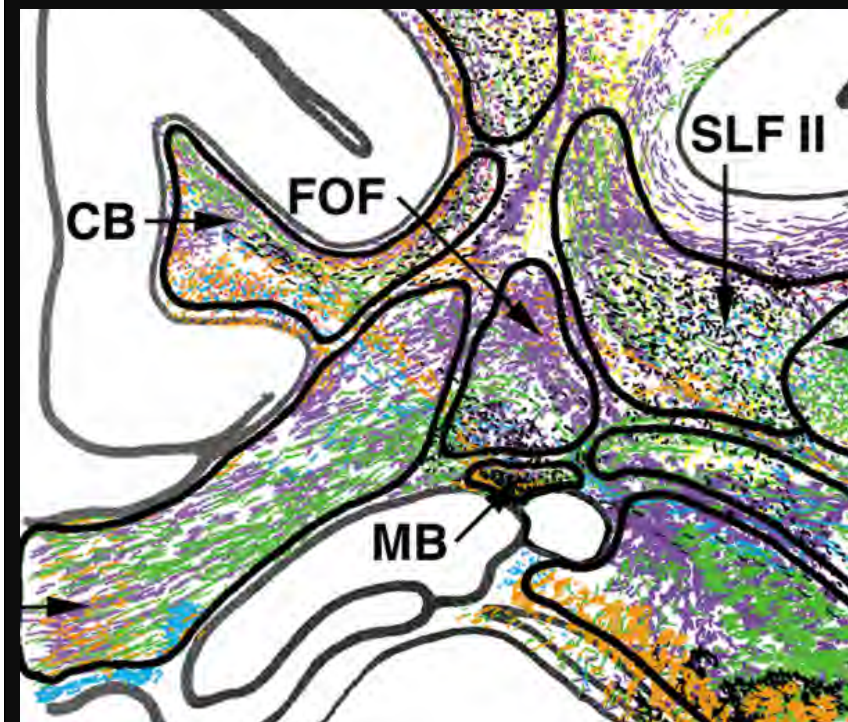

DSI - 6D

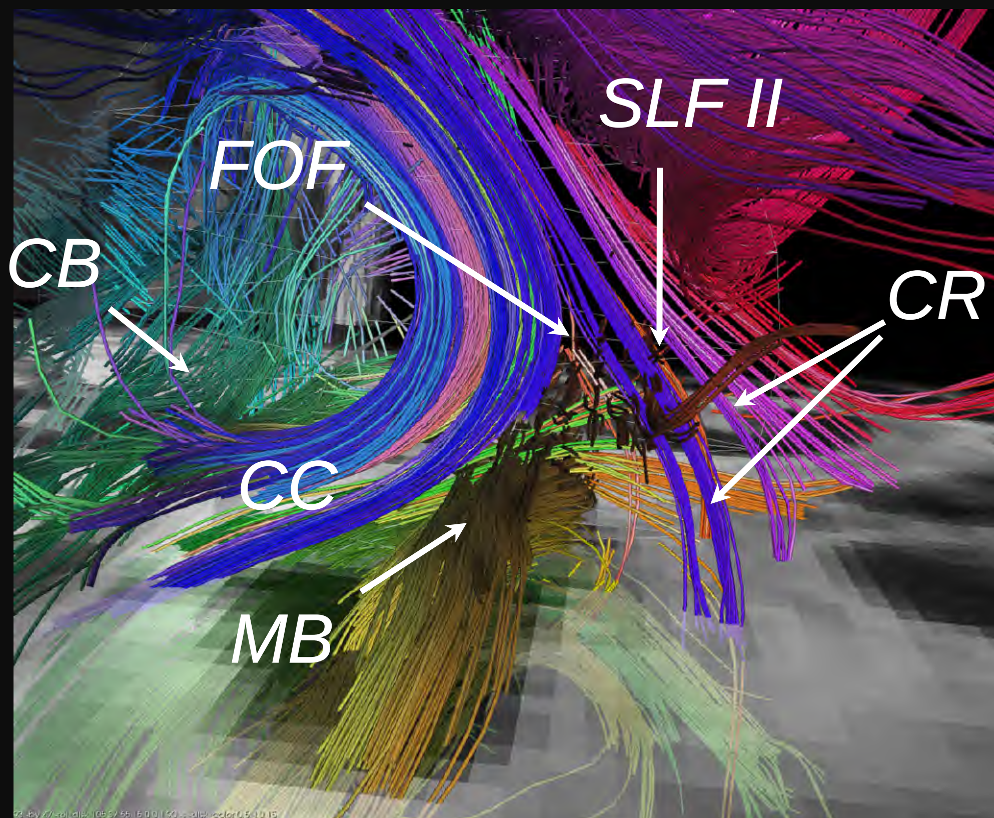

Schmahmann et al Brain 2007

Macaque centrum semiovale

DTI

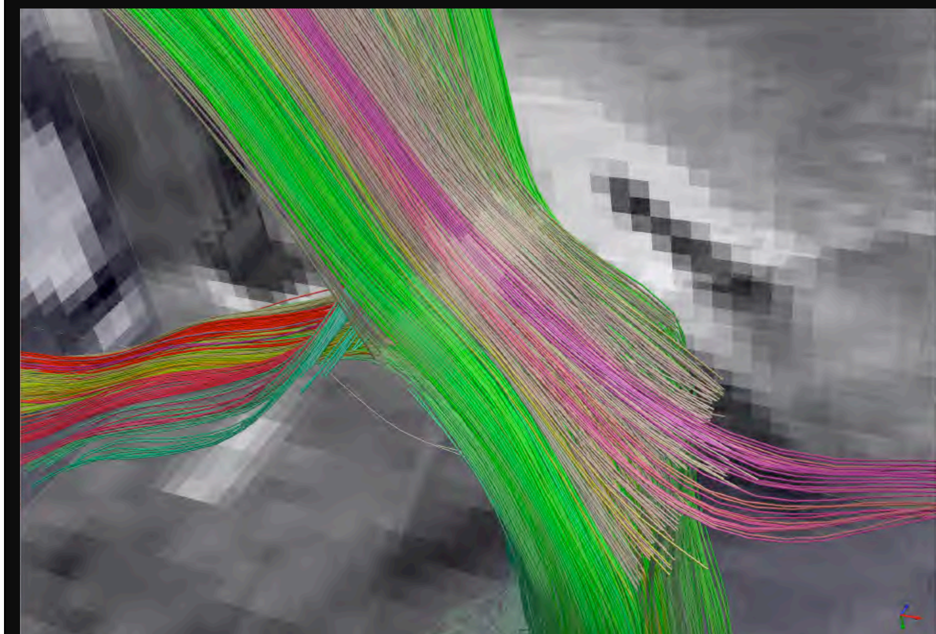

DSI

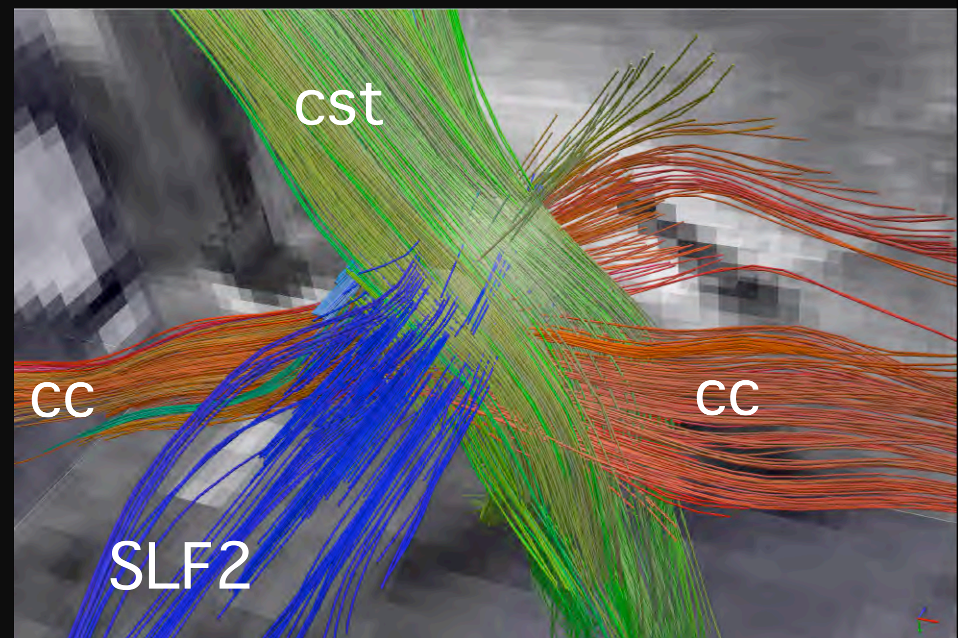

Validation DSI and tracer rhesus SLF3

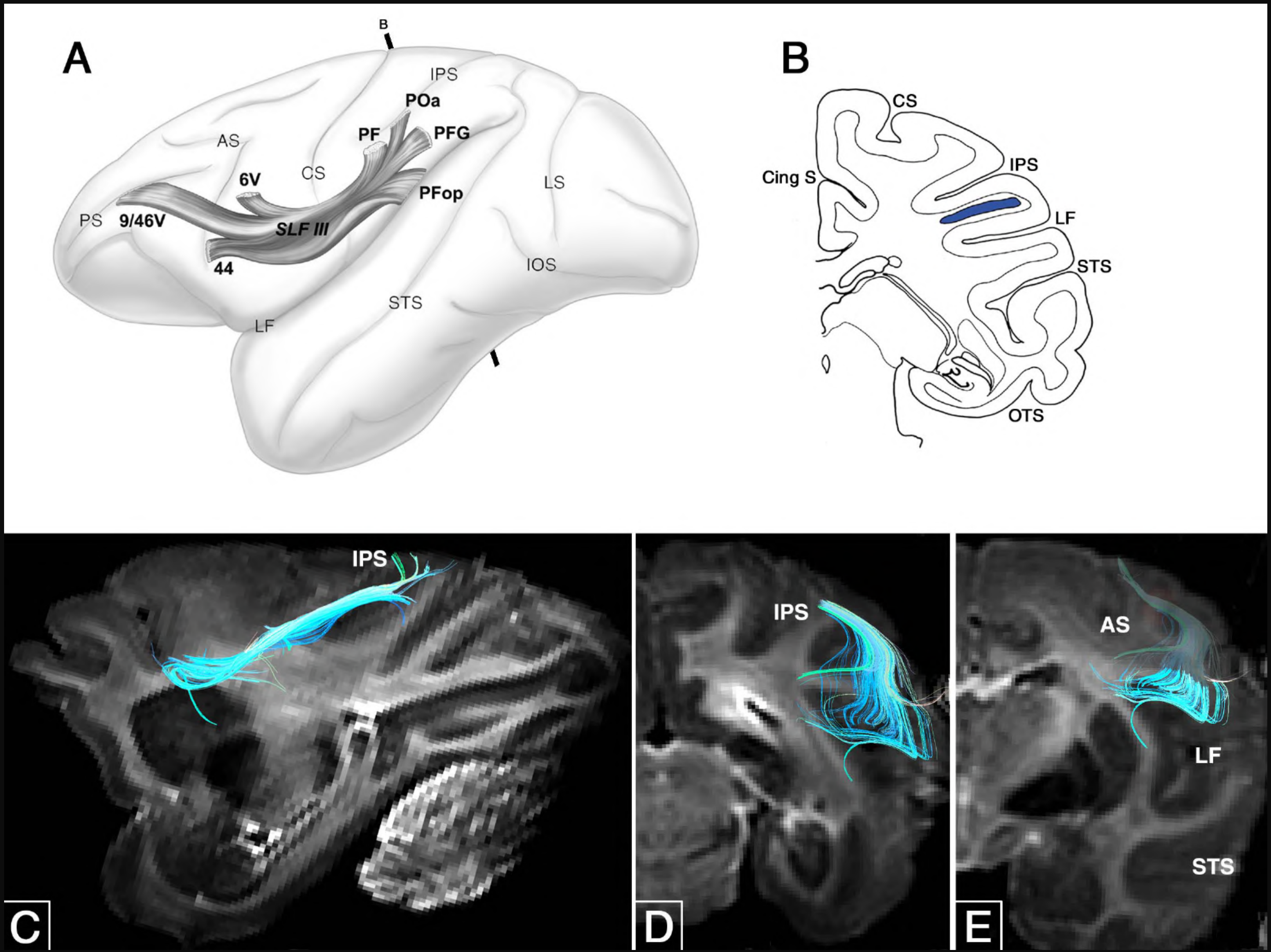

DSI connectivity of macaque superior frontal gyrus

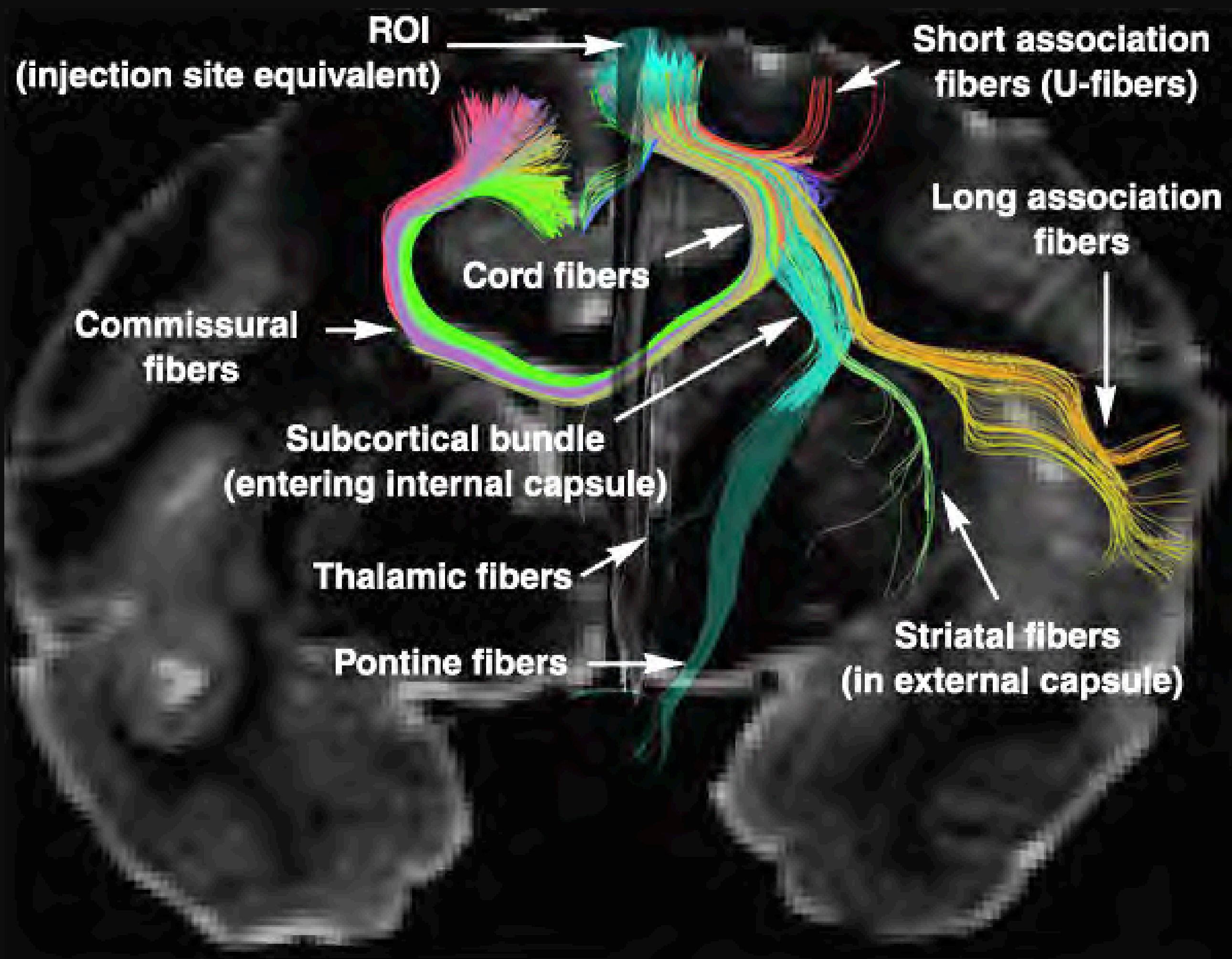

Schmahmann JD, Pandya DN, Wang R, Dai G, D'Arceuil HE, de Crespigny AJ, Wedeen VJ

DSI rhesus BA10 connectivity

tracer Petrides & Pandya

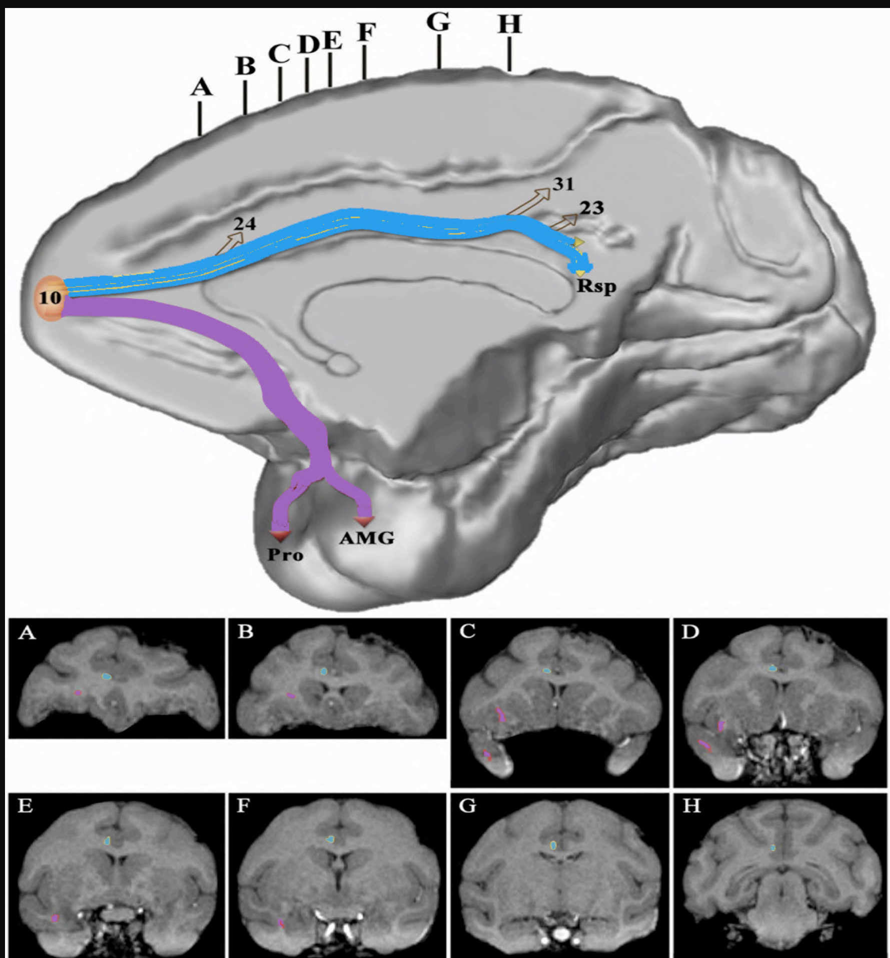

DSI

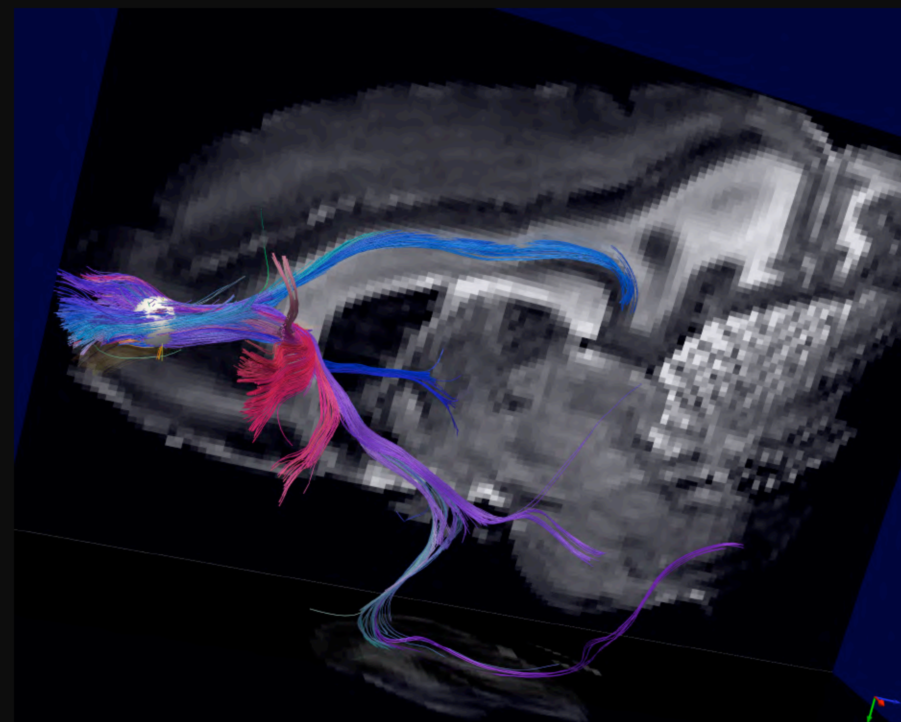

Macaque

MRI 3D and overlap

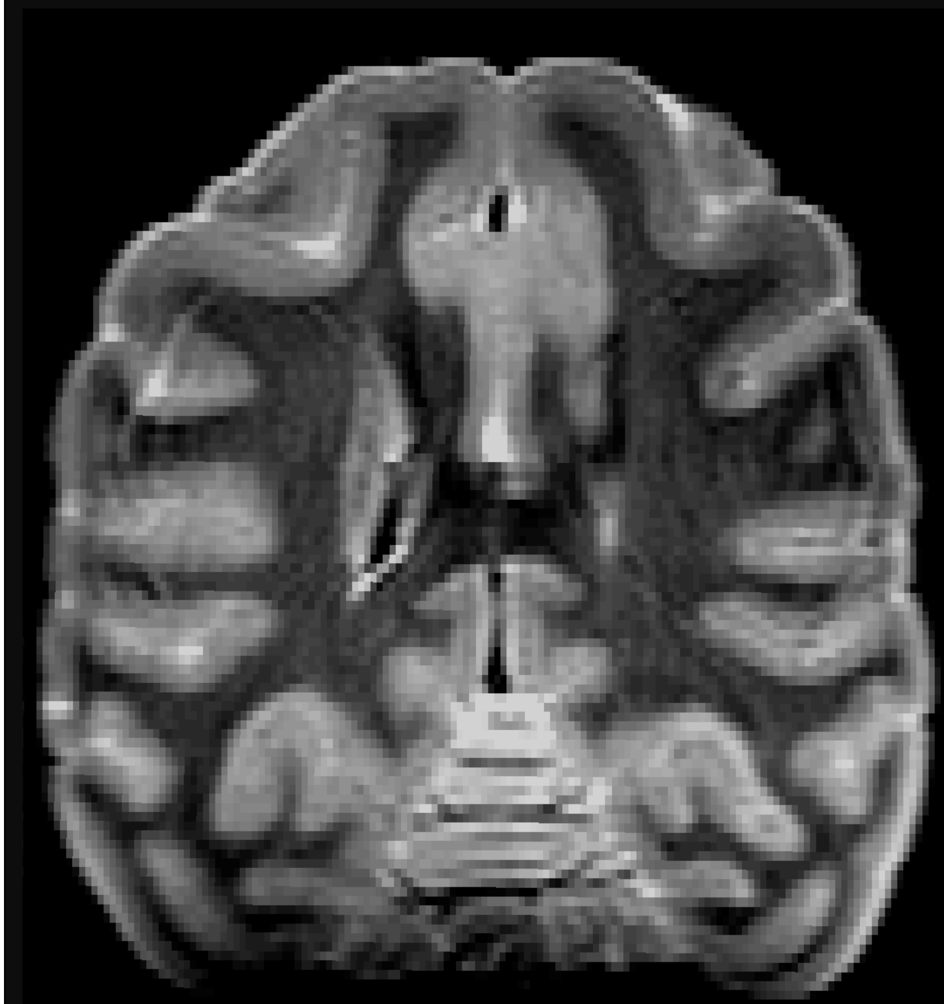

DSI 6D and no overlap

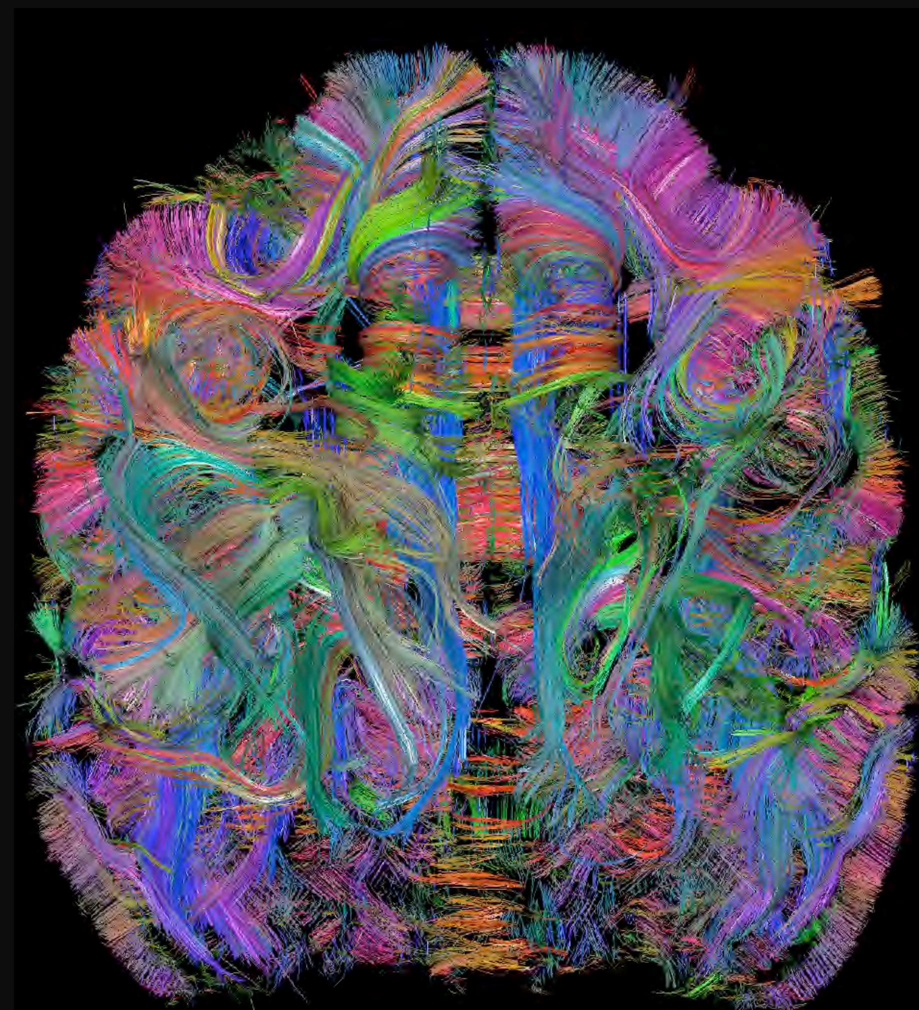

DSI human connectome - Hagmann et al PLoS Biol 7.08

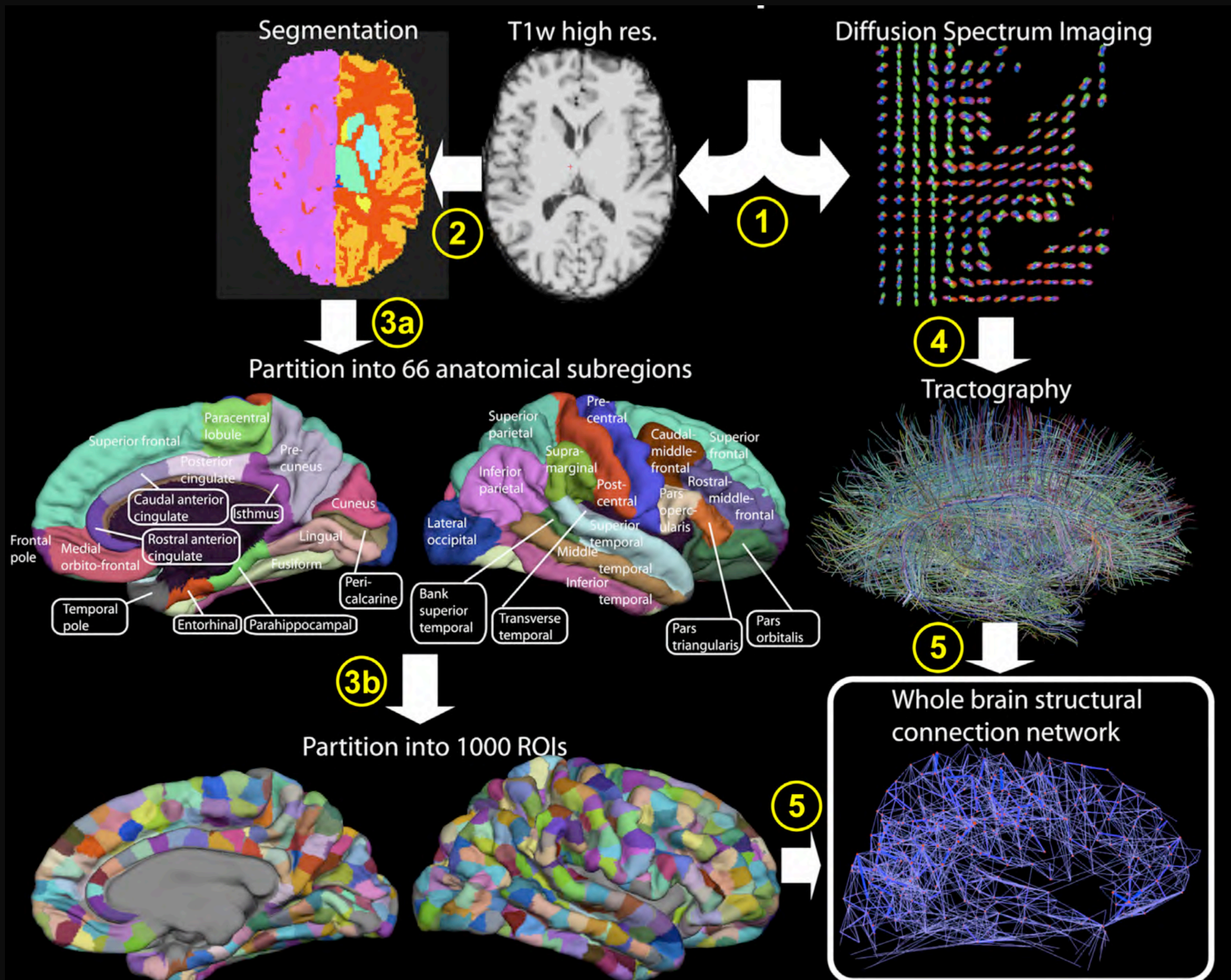

Macaque connectome
DSI and CoCoMac

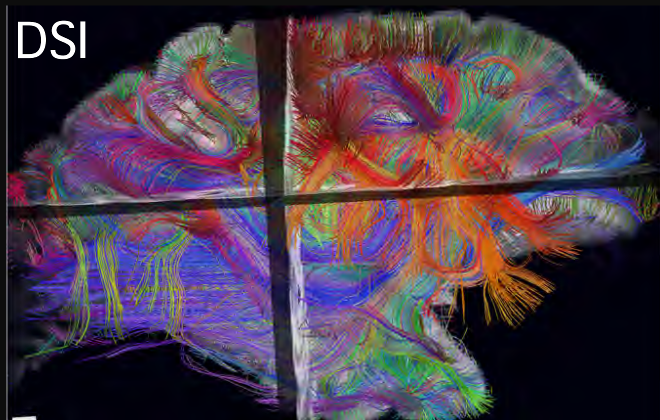

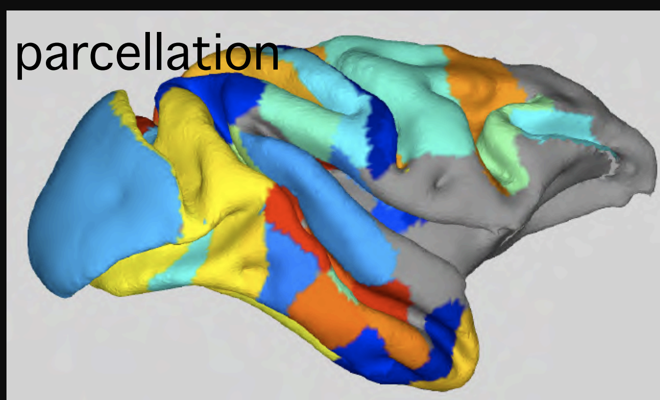

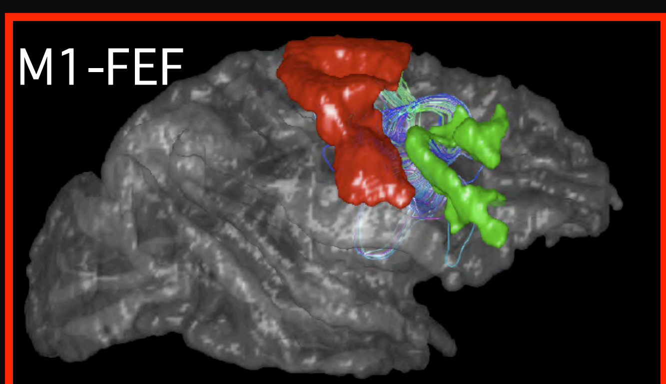

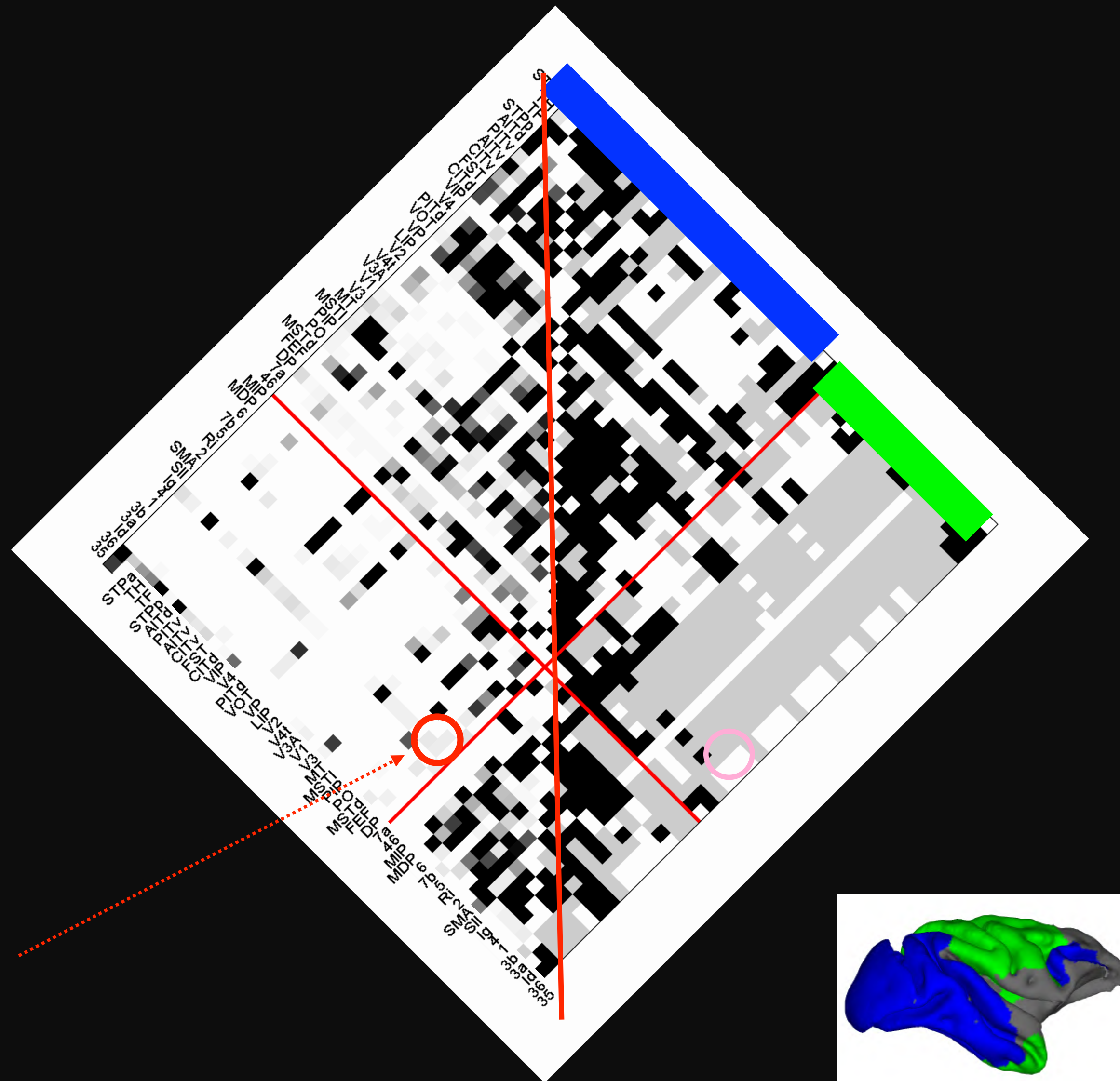

Hagmann PLoS Biol 2008

DSI in vivo human

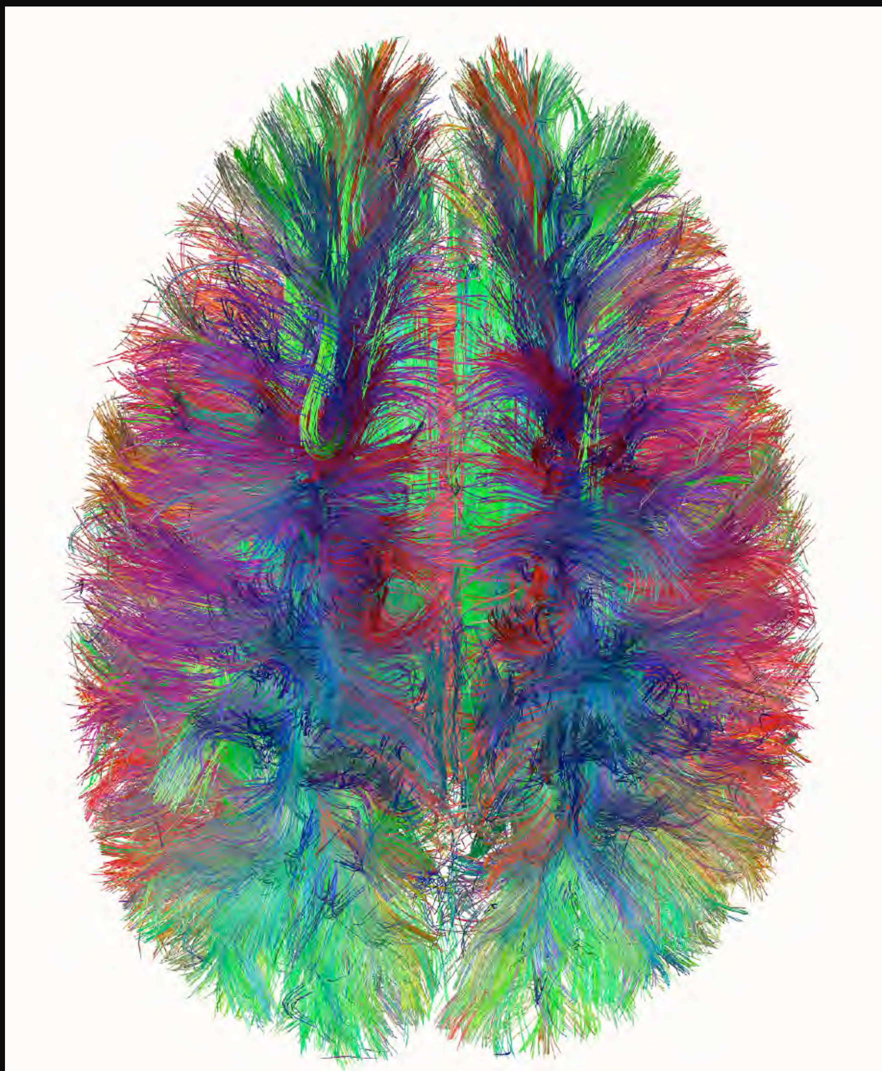

human connectome

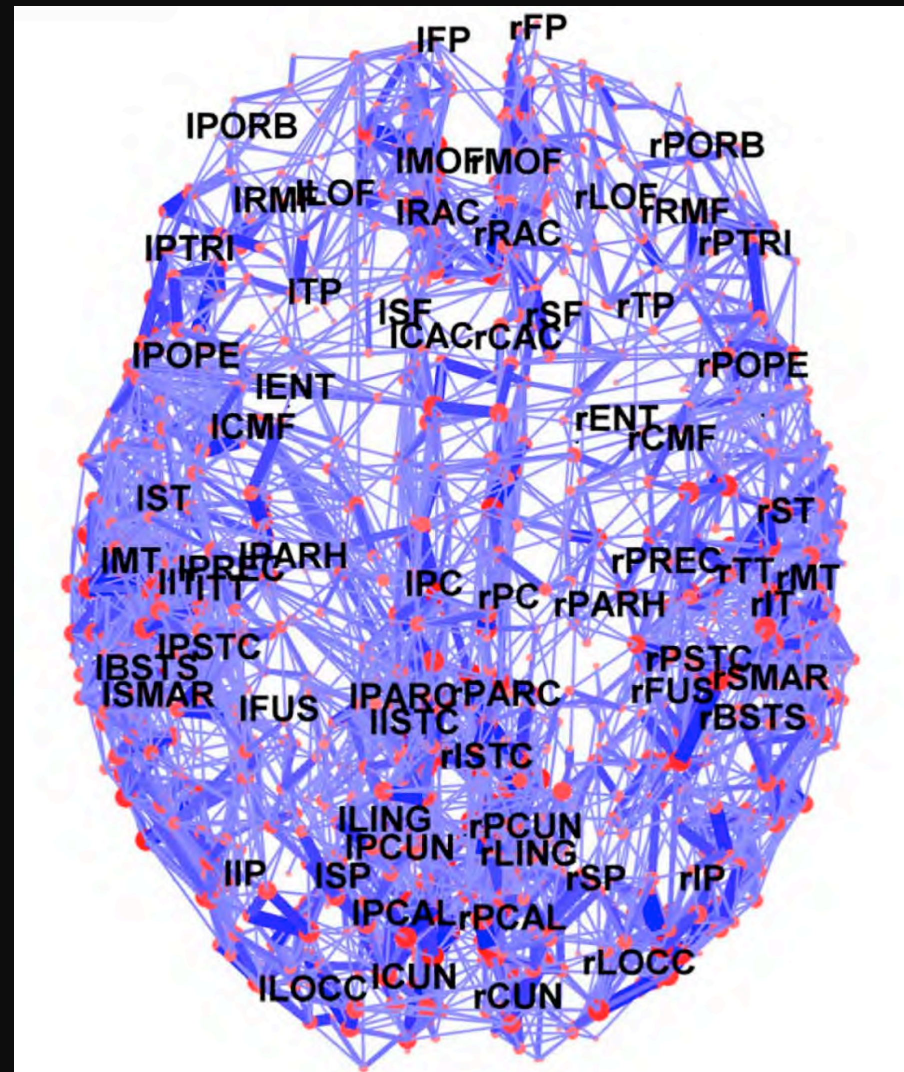

Hagmann et al PLoS Biol 2008

Human connectome hubs and core

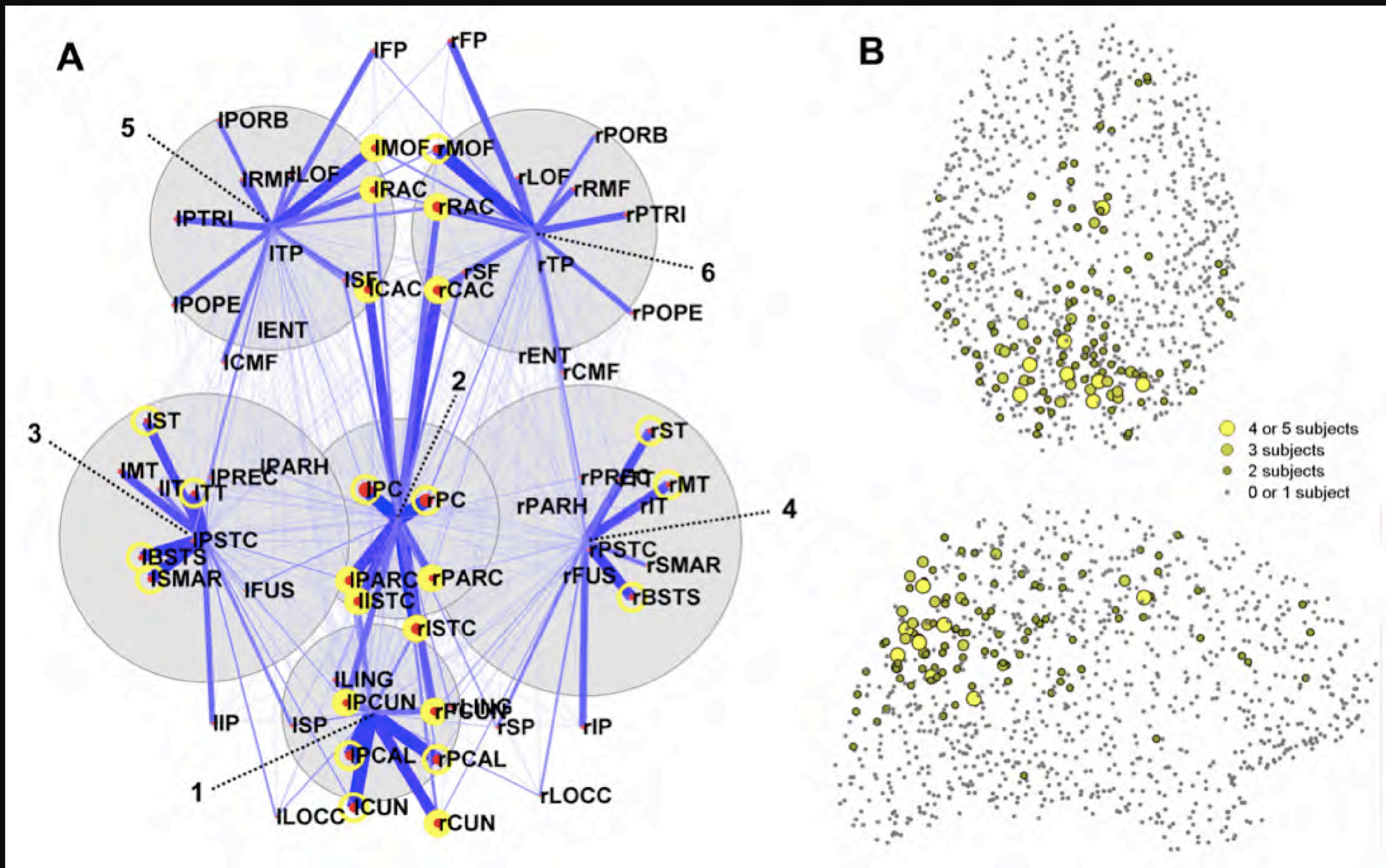

Hagmann et al PLoS Biol 2008

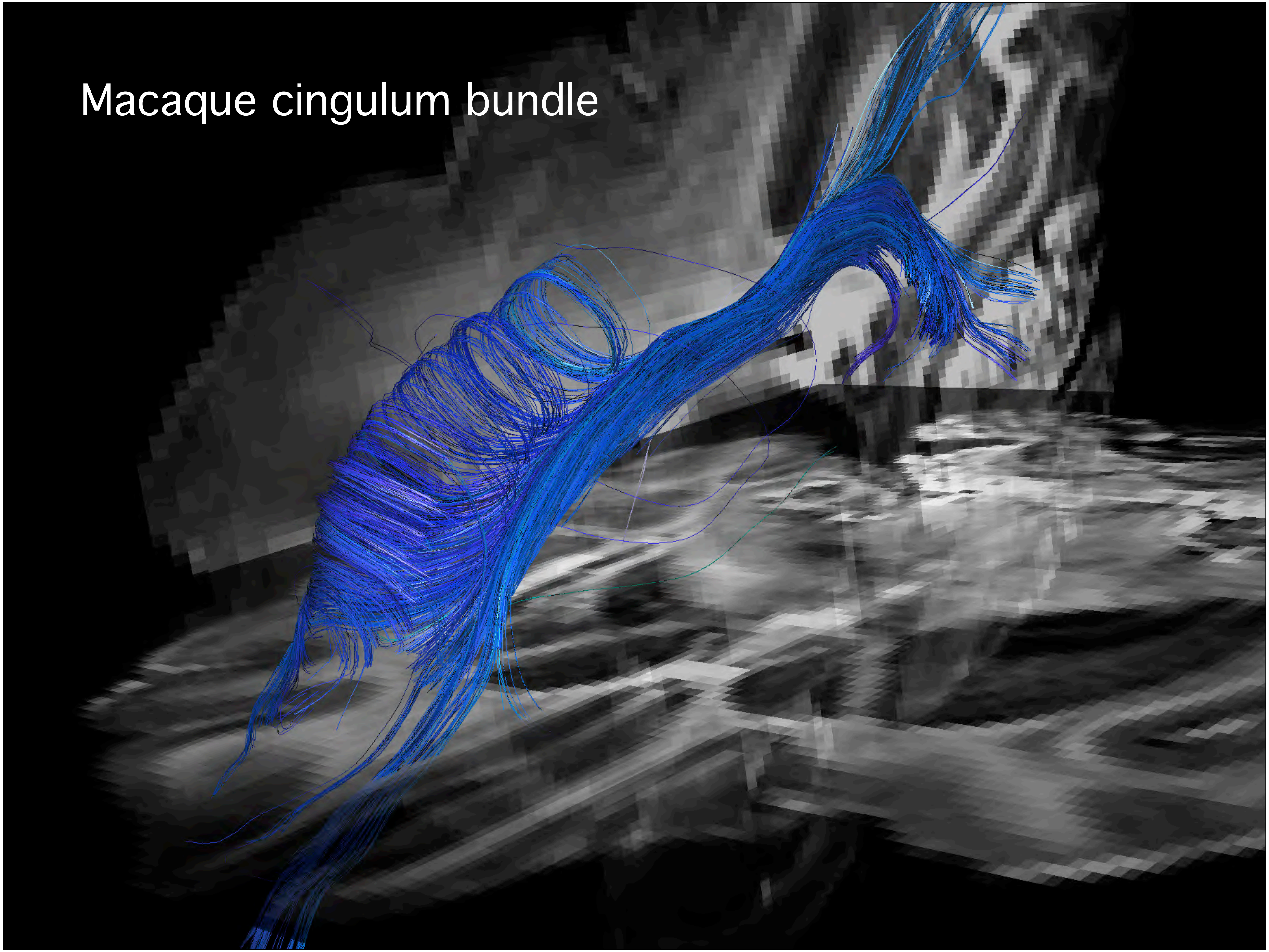
Macaque cingulum bundle

Human hippocampus ex vivo DSI digital dissection

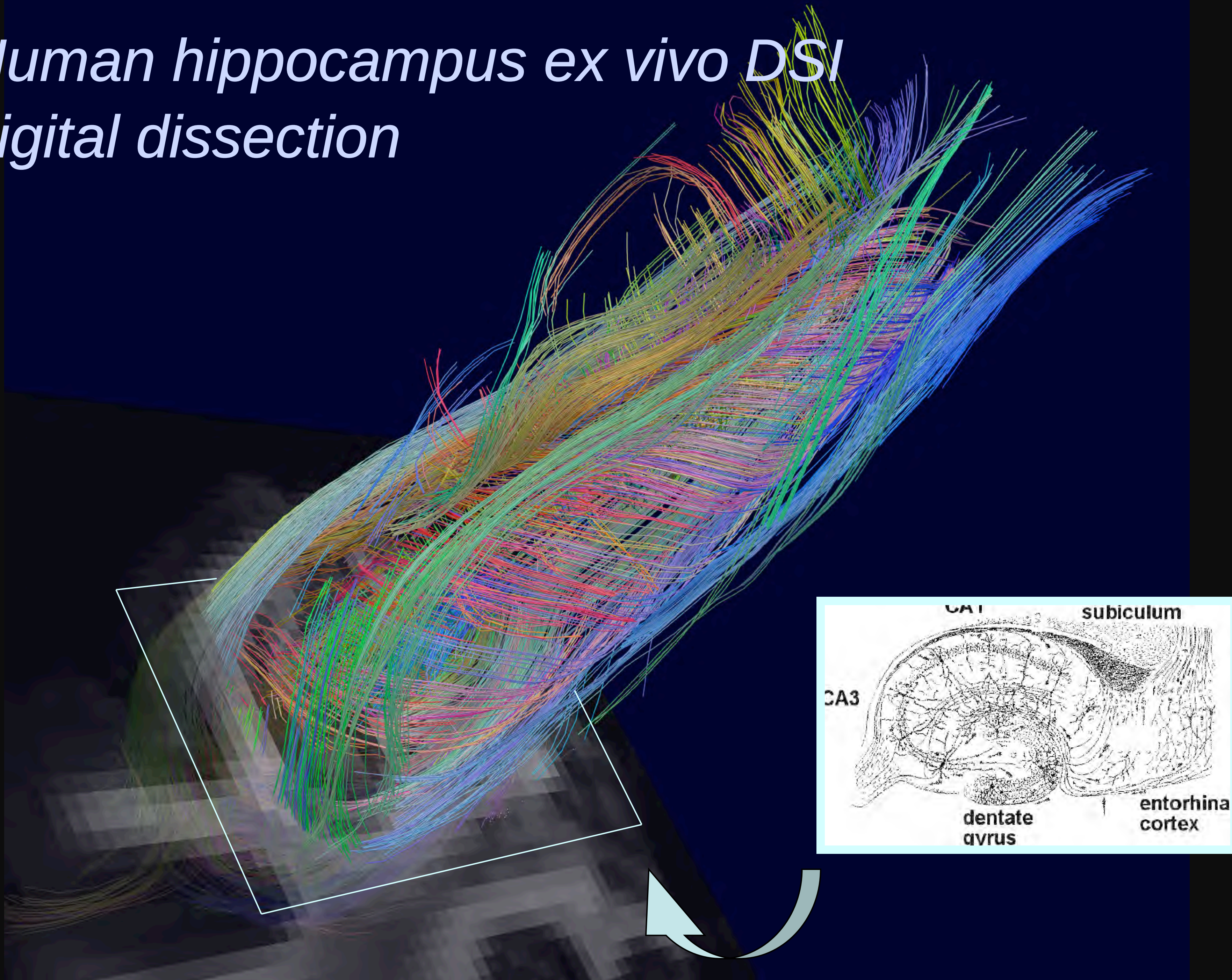

Macaque calcarine connections

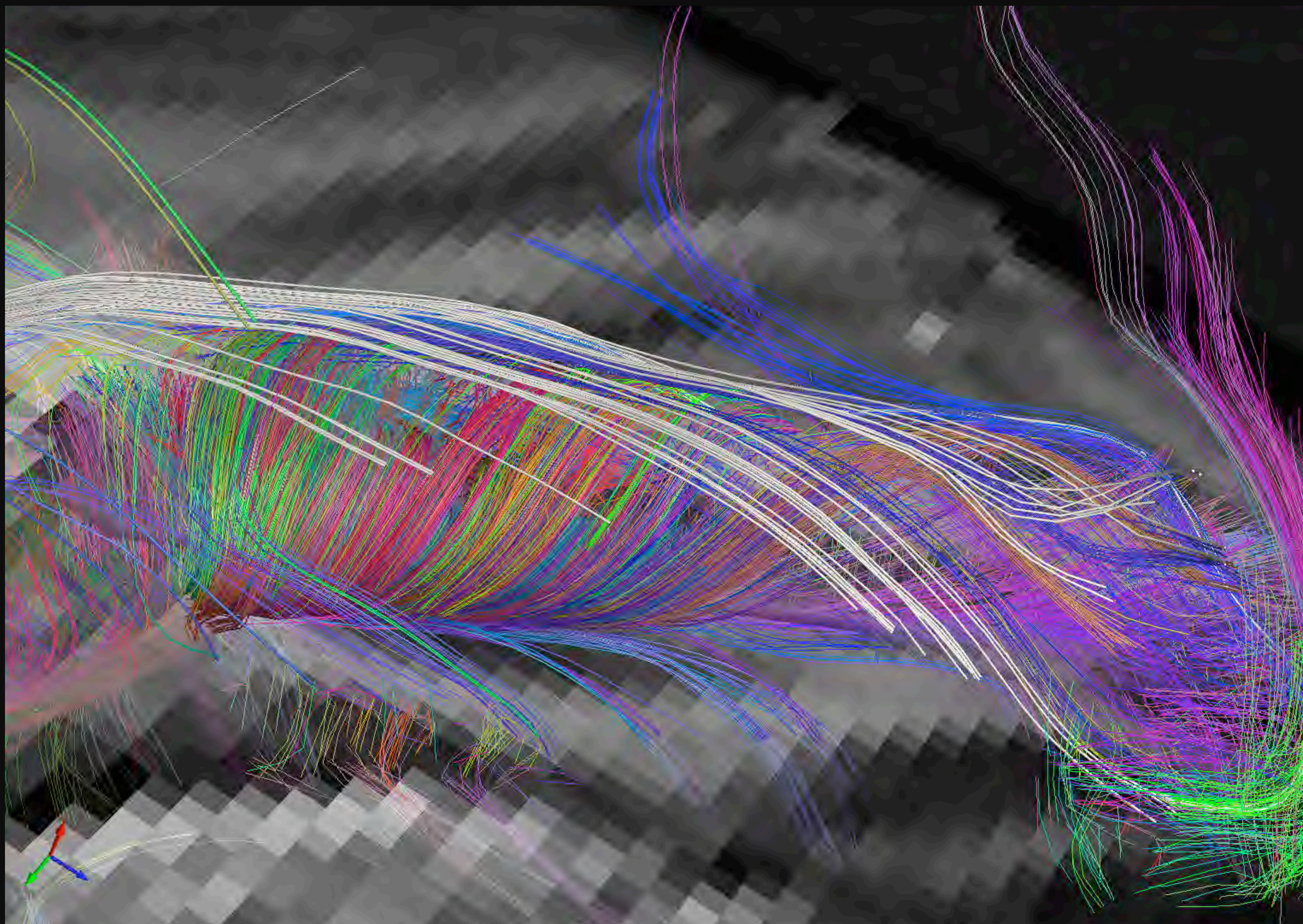

Early evidence of geometric structure, owl monkey hippocampus 2005

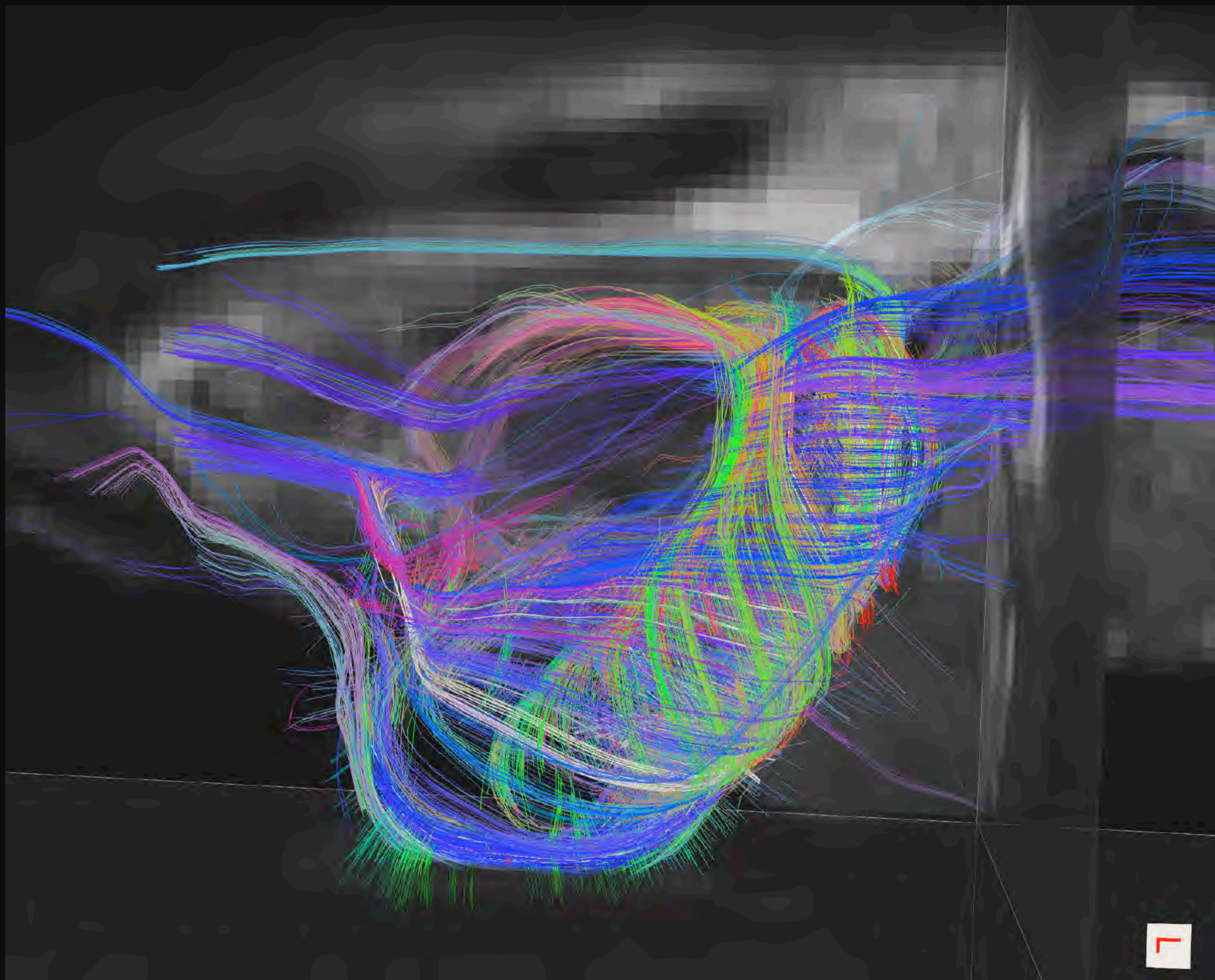

Human cortex 300u

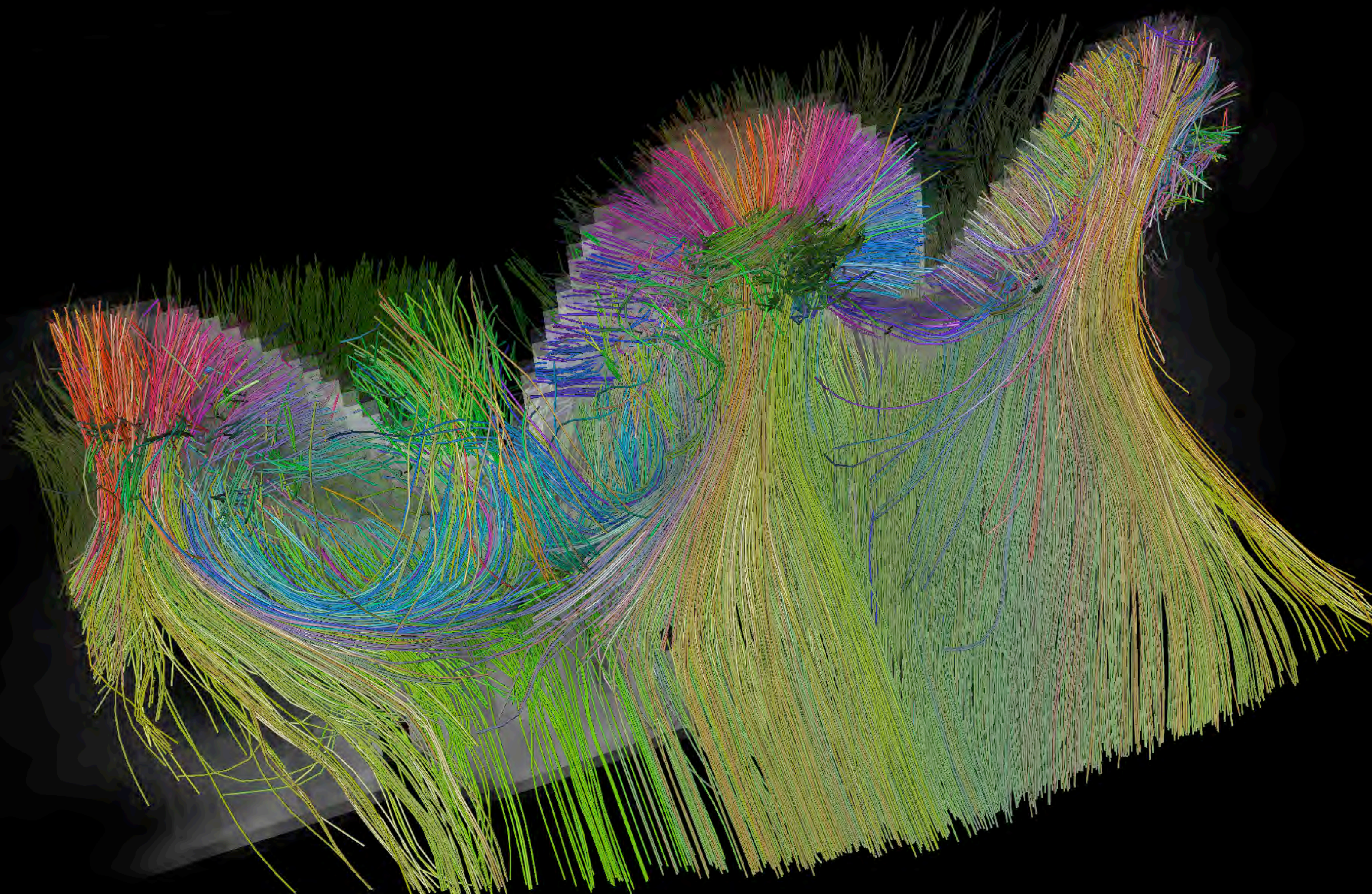

human_cortex_smoothed_skipp_10. -roi standard_dwi.img -ext 1 -roi_th 200 -b standard_dwi.img -w 1 3000 -by 23 -ny 23 -nx 37 64 -s

Approach to "diffusion resolution"

The aim of diffusion MRI is to image an underlying shape.

This is limited by blurring from 2 sources:

- blurring due to finite resolution of the diffusion camera

$$1/q_{max} = 1/GT$$

- burring due to diffusion itself

$$\sqrt{2DT}$$

Combining these, overall diffusion resolution R is

$$R^2 = (1/GT)^2 + 2DT$$

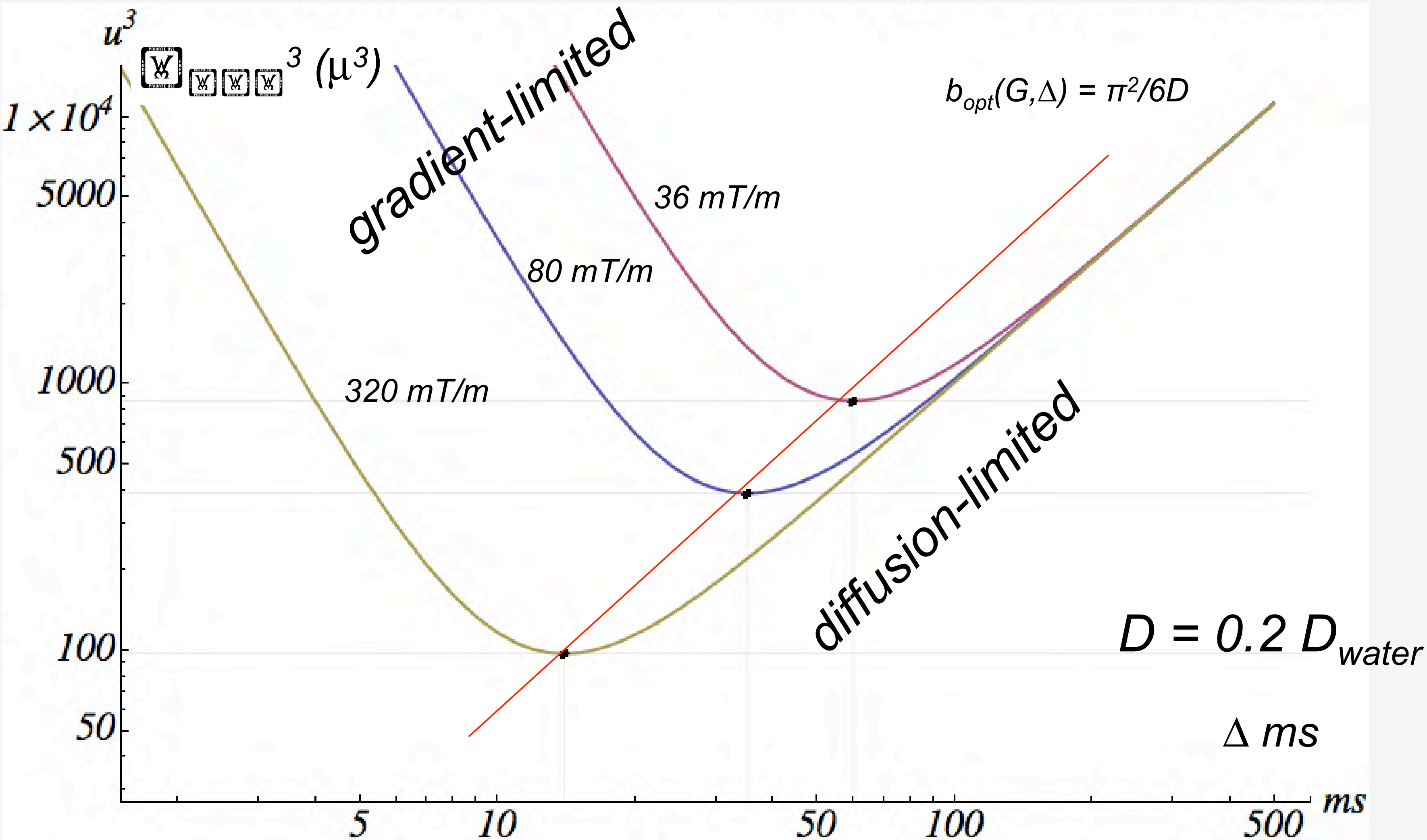

u3
3 (μ3)
gradient-limited
bopt(G,Δ) = π2/6D
36 mT/m
80 mT/m
320 mT/m
diffusion-limited
D = 0.2 Dwater
Δ ms
1 × 10^4
5000
1000
500
100
50
5
10
50
100
500
ms

Consequences:

For any gradient G, there is a best-possible micro-resolution

$$R_{eff} = (D/G_{max})^{1/3}$$

For any diffusion D_{min}, there is a universal optimum b-value

$$b_{opt} = \pi^2/6D_{min}$$

In astronomy, the way to sensitivity and resolution is mirror diameter

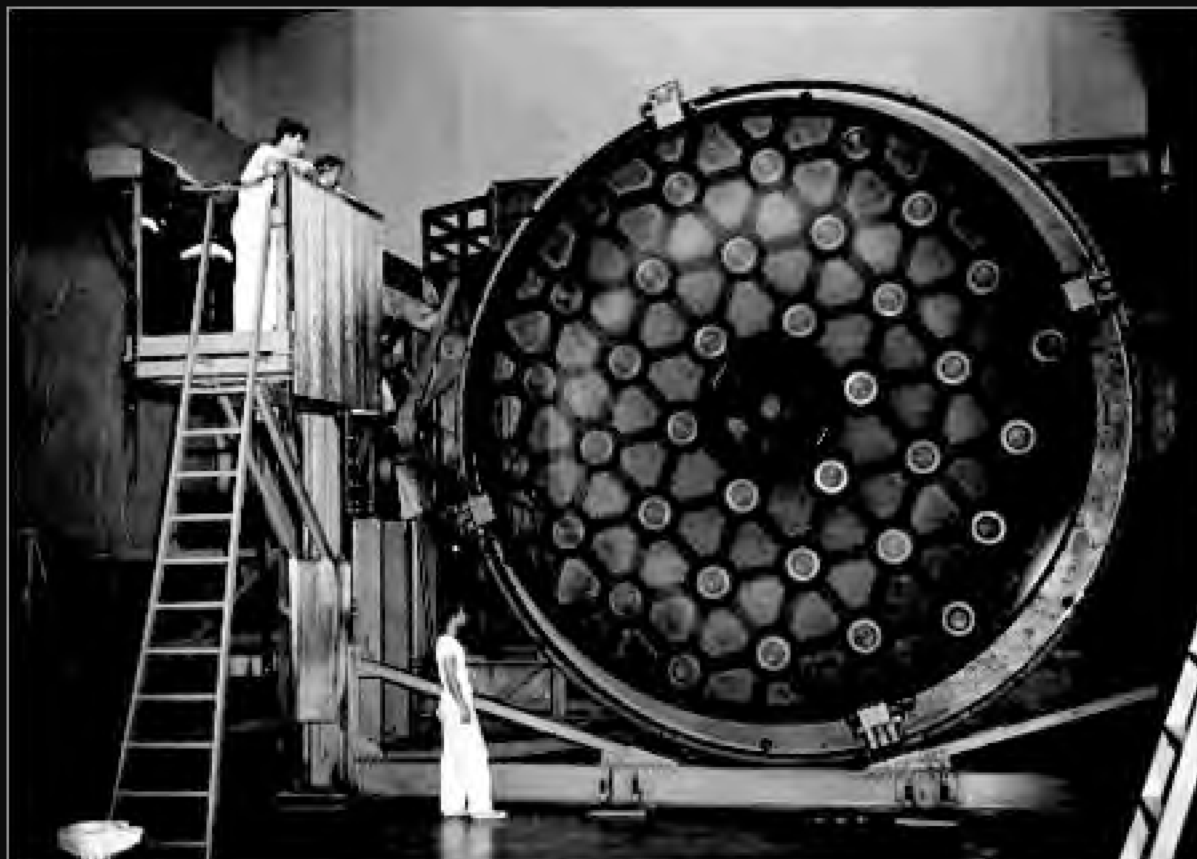

Corning 200" mirror for the Hale Telescope at Mt Palomar

In diffusion MRI, the way to boost signal-to-noise and resolution of micro-structure is gradient strength

MGH-UCLA HCP

Immediate goal: map human connectivity

Long-term goal: objective mental health care

NIH **Blueprint** for Neuroscience Research

The ultimate diffusion machine…

7x the gradient strength.

G_{max} = 300mT/m

Slew = 200 T/m/s

4x the encoding speed.

(thru simultaneous multi-slice imaging)

64 channel brain array

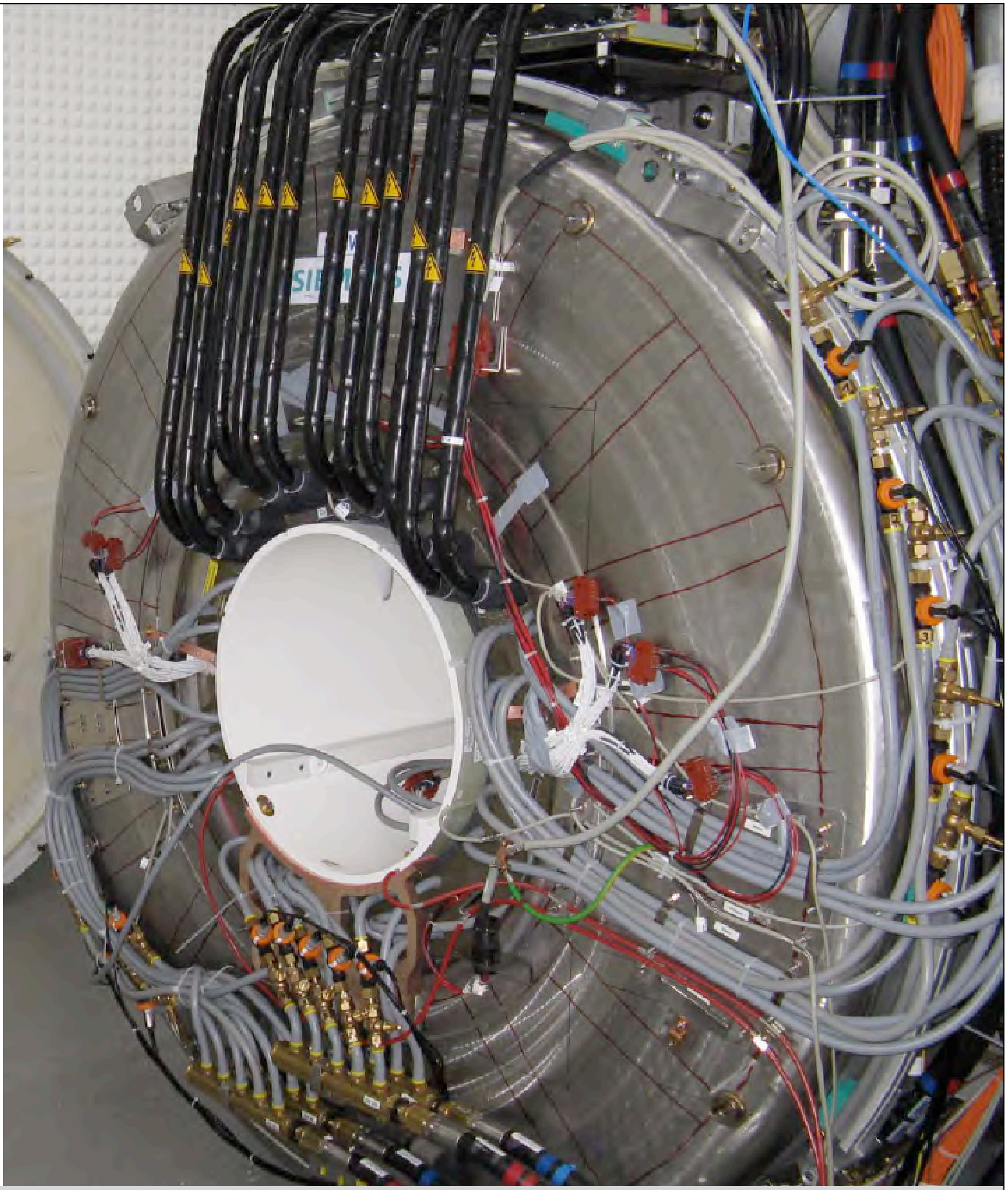

Expect nearly 10x increase in sensitivity for high b value diffusion

The MGH Connectom Scanner

Compared to Skyra-GC:
4x gradient amplifiers
4x external gradient connections
4x times water cooling layers
2x layers per gradient axis
8x times the peak
gradient strength 300mT/m!

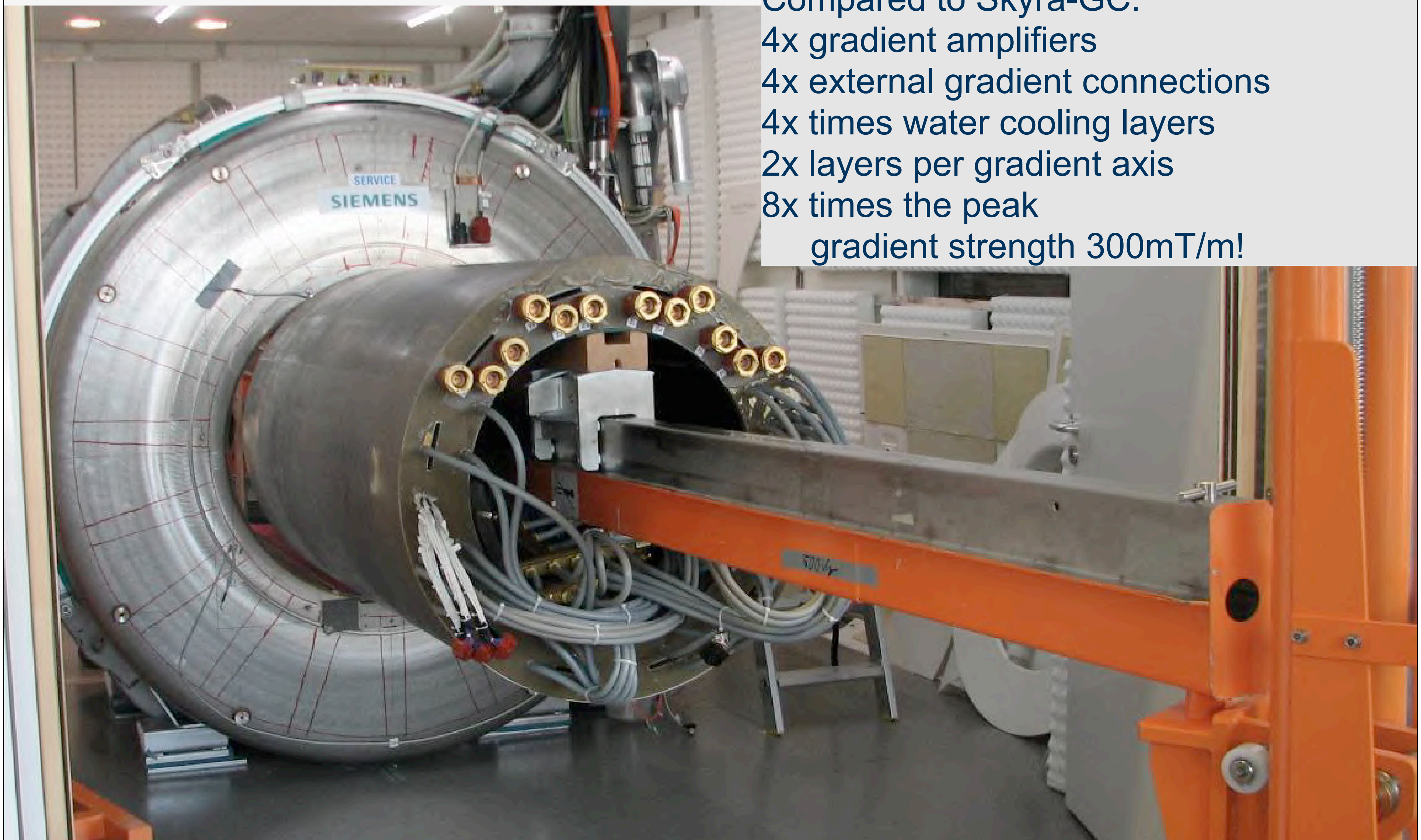

3T Connectom scanner, 24 megawatts
Los Angeles class nuclear submarine, 26 megawatts

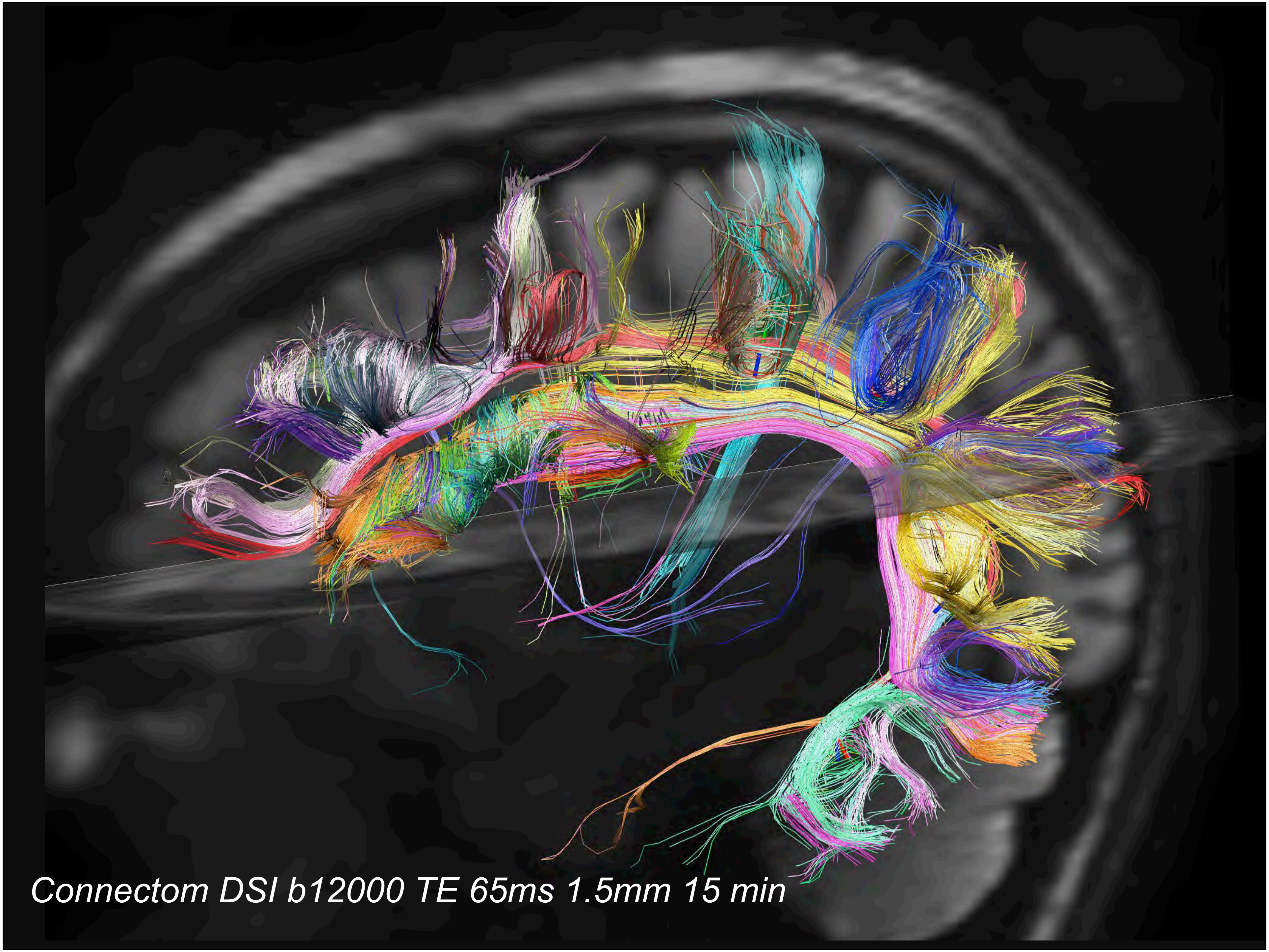
Connectom DSI b12000 TE 65ms 1.5mm 15 min

Van Wedeen
Ellen Grant
Doug Rosene
Patric Hagmann
Jon Kaas
W-Y Isaac Tseng
Larry Wald
Ruopeng Wang
Bruce Rosen
Guangping Dai
and
Farzad Mortazawi
Thomas Witzel

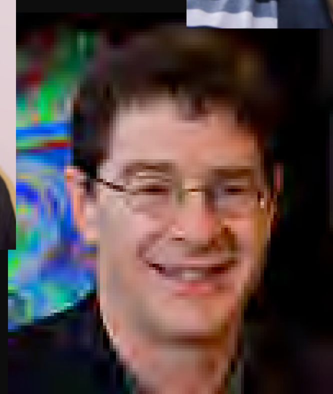

Cat DSI

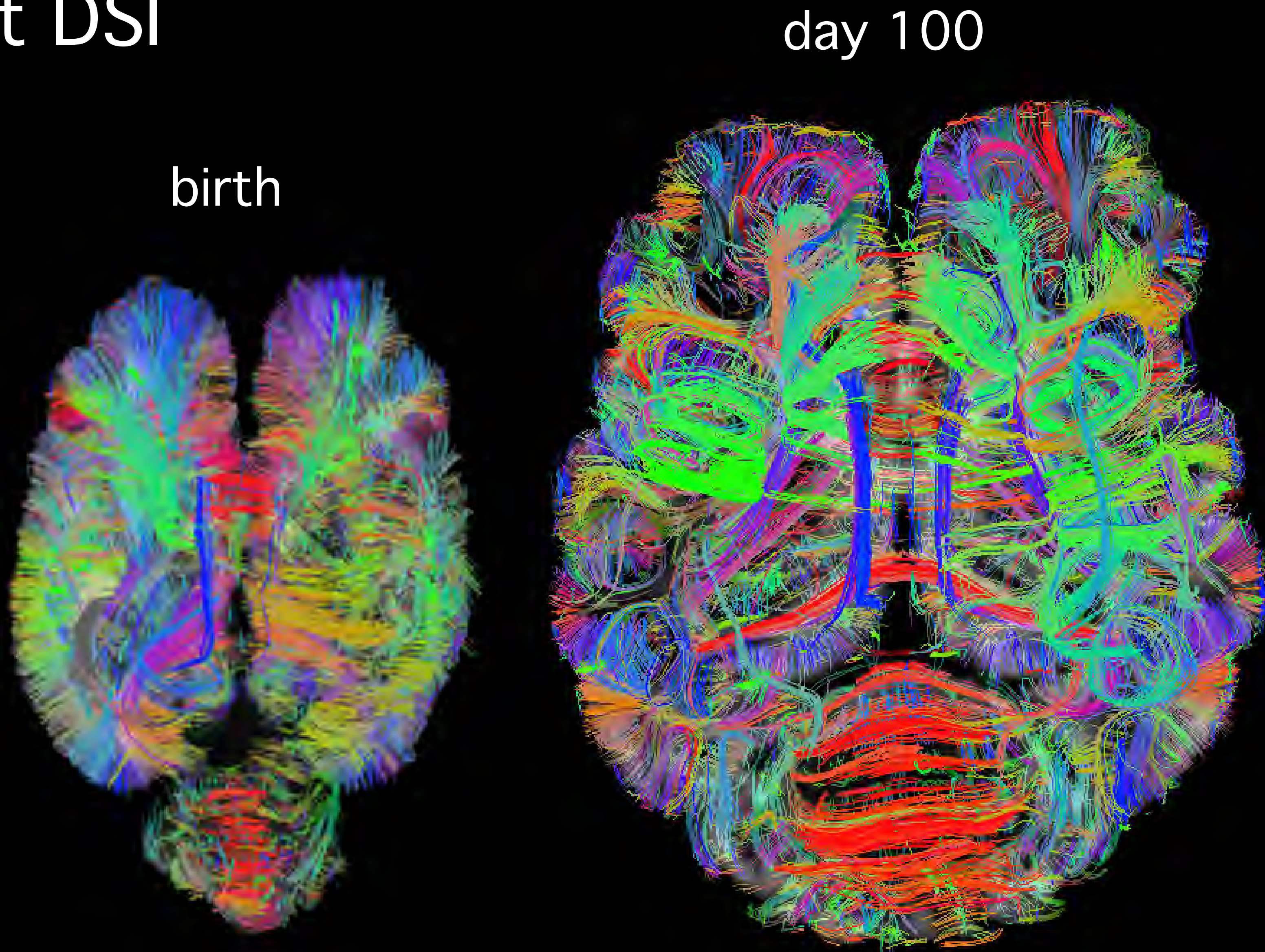

Takahasi et al ISRMR 2008

DSI Connectom 1.5mm b15k TE 68ms 15 min

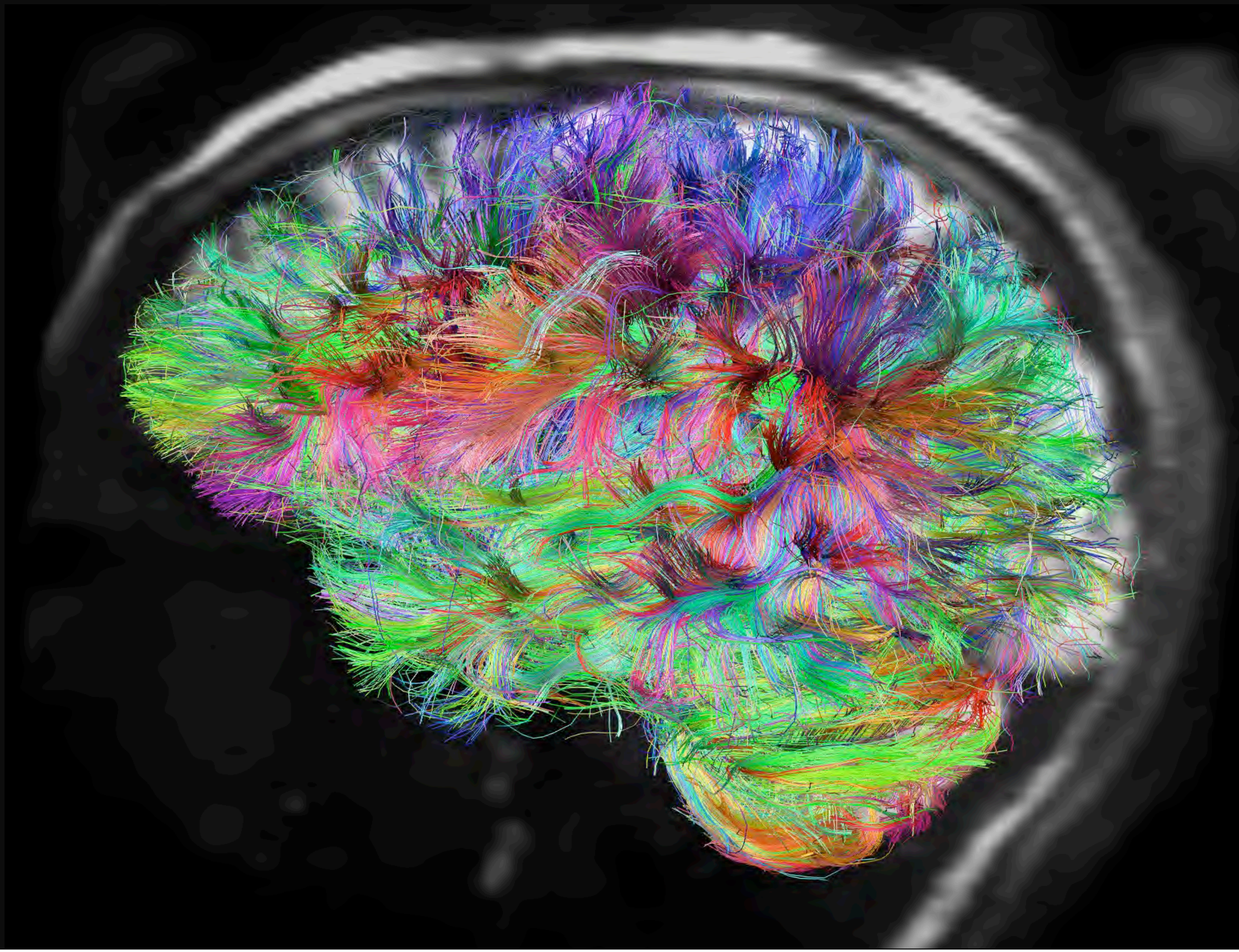

Cat cortico-thalamic tracts development

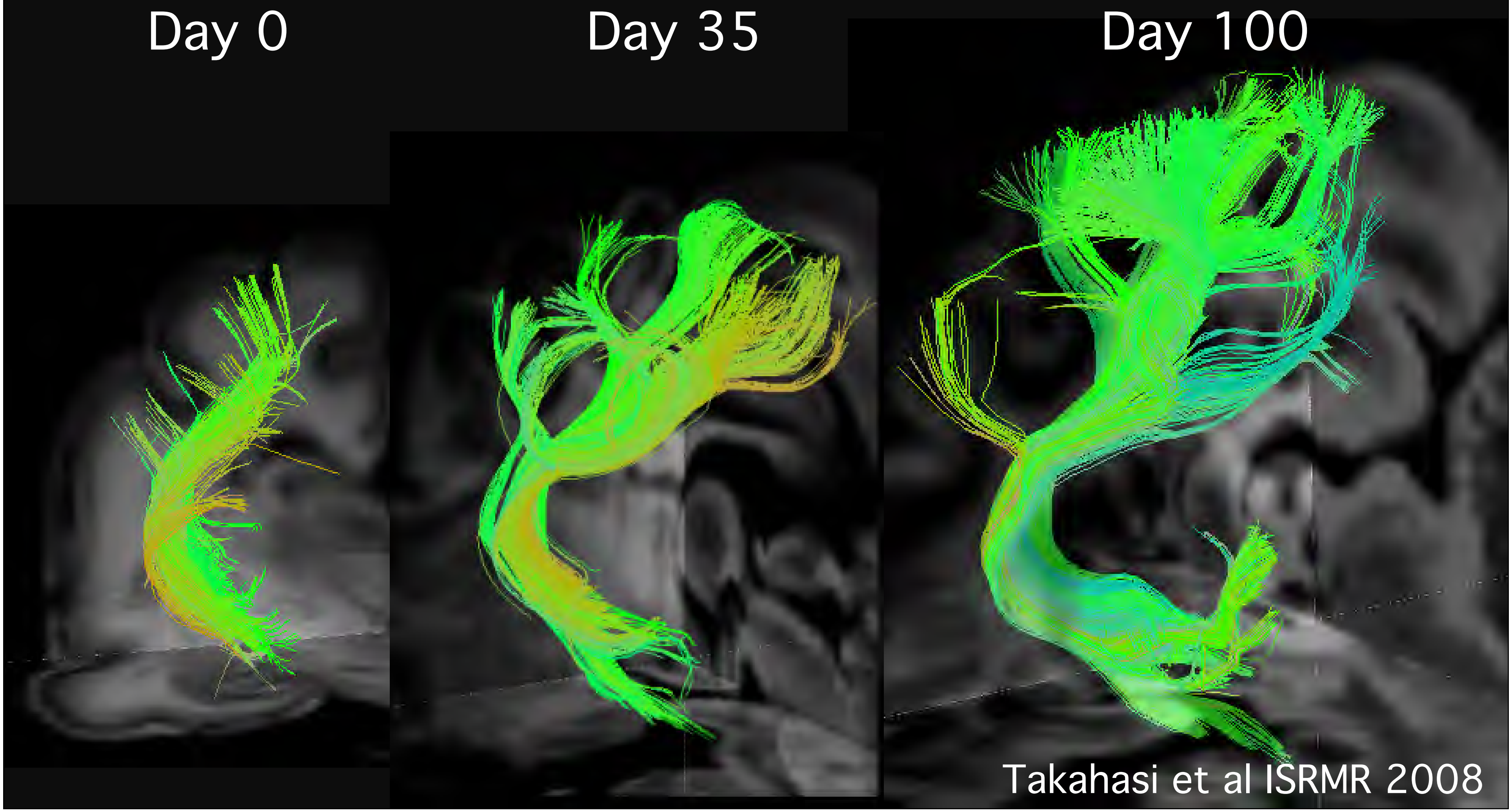

Human cortex specimens

normal control vs. polymicrogyria

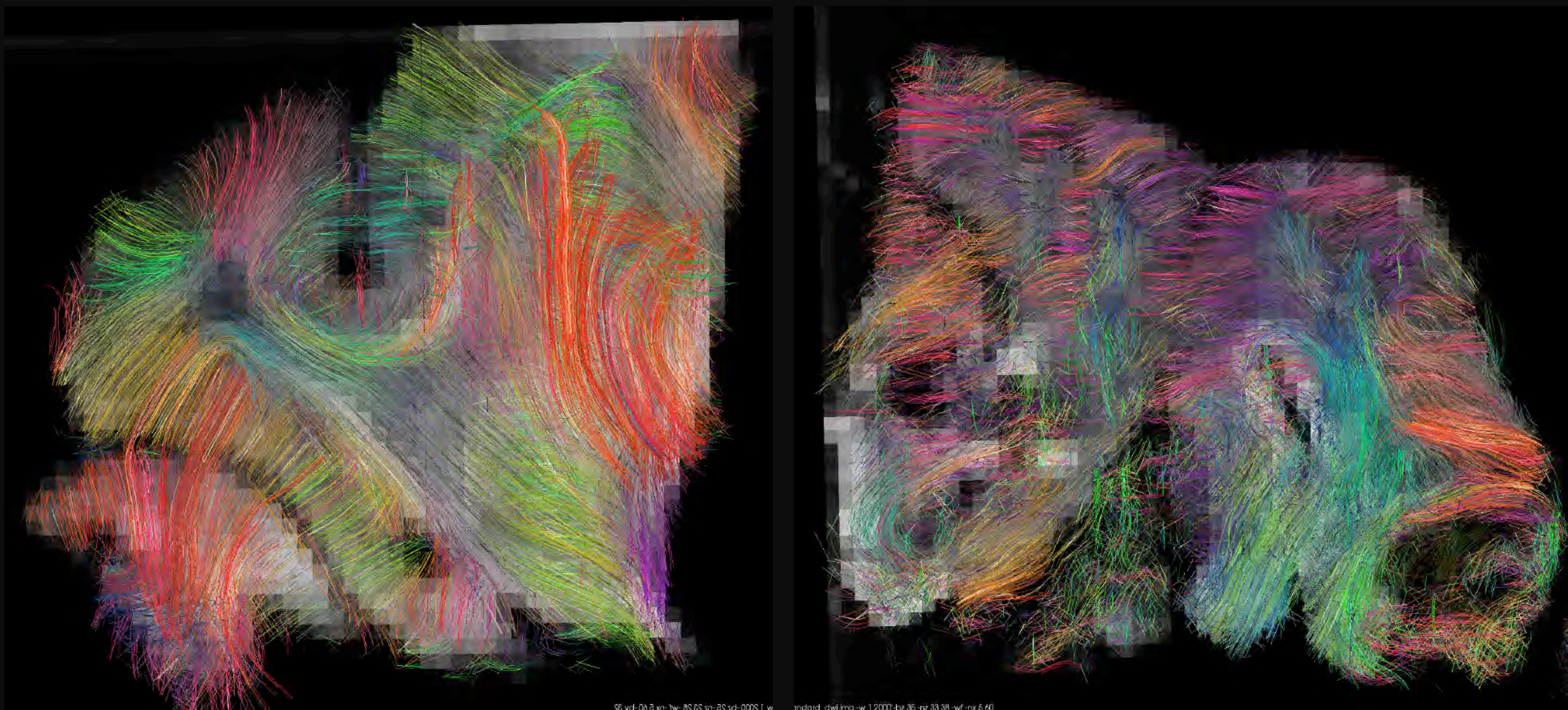

Ellen Grant, RP Wang, A deCrespigny, VJ Wedeen - MGH Radiology

Intracortical connectivity

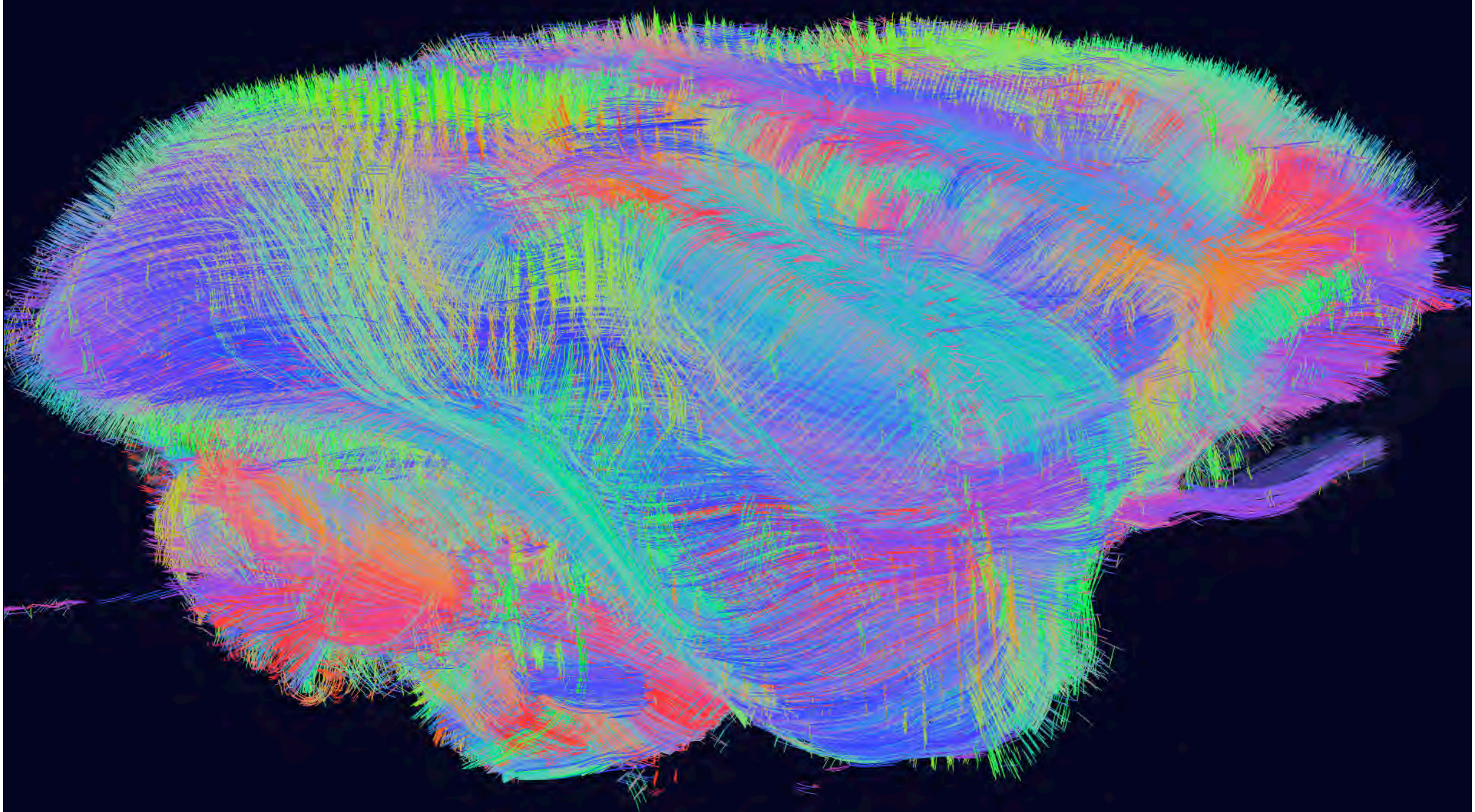

Cat and mouse

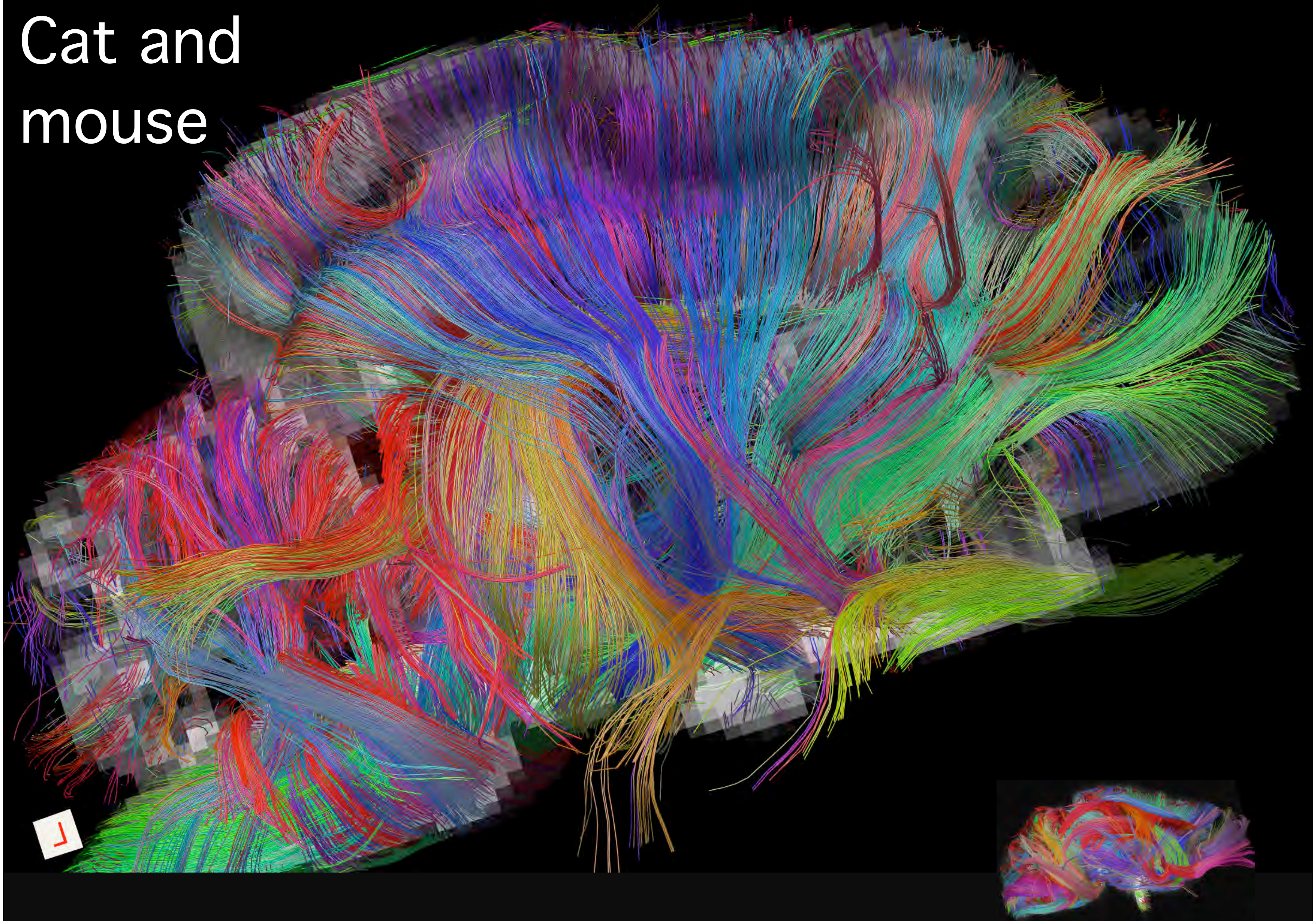

Macaque circuit of Papez ex vivo

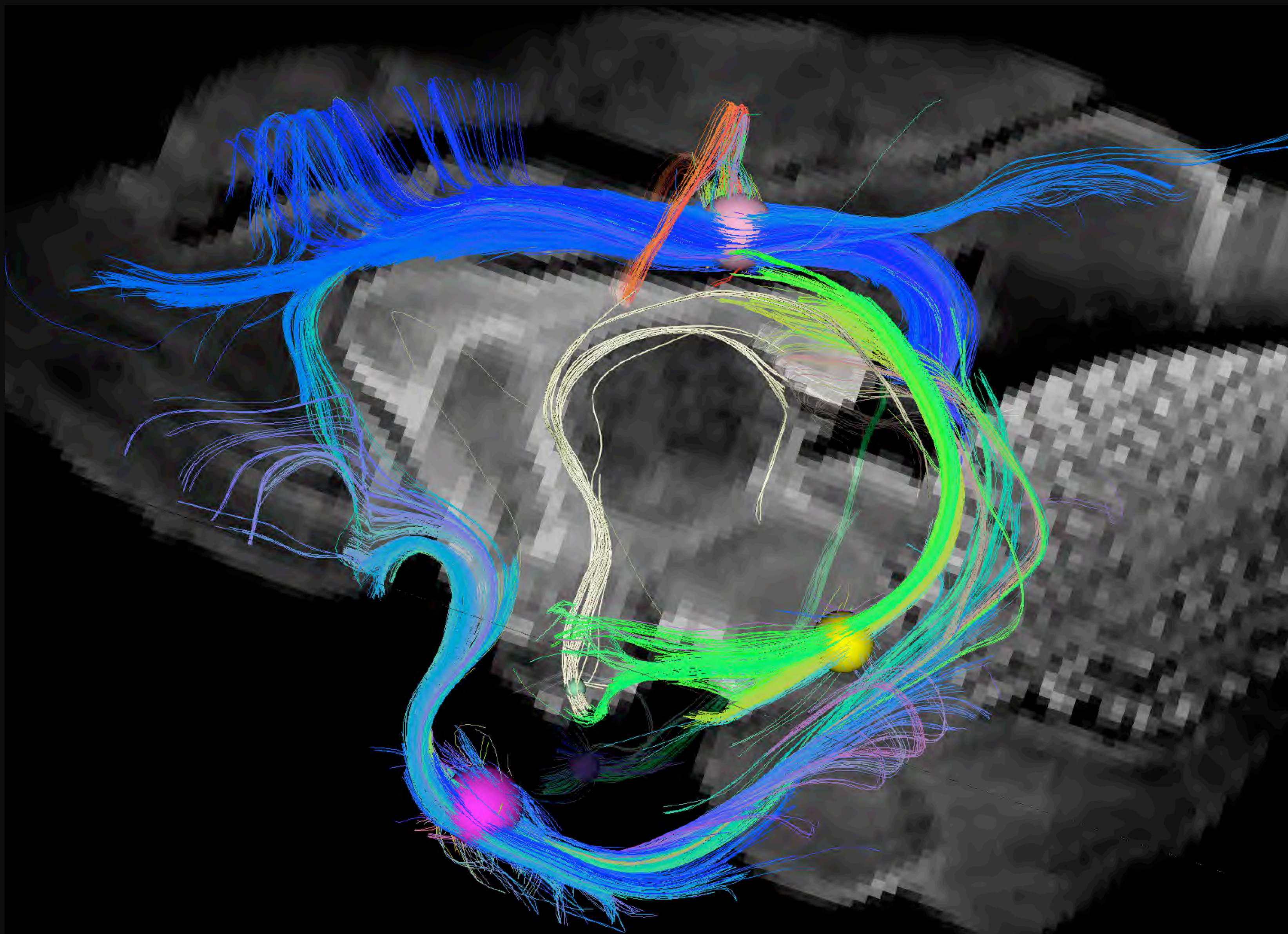

Human pons ex vivo

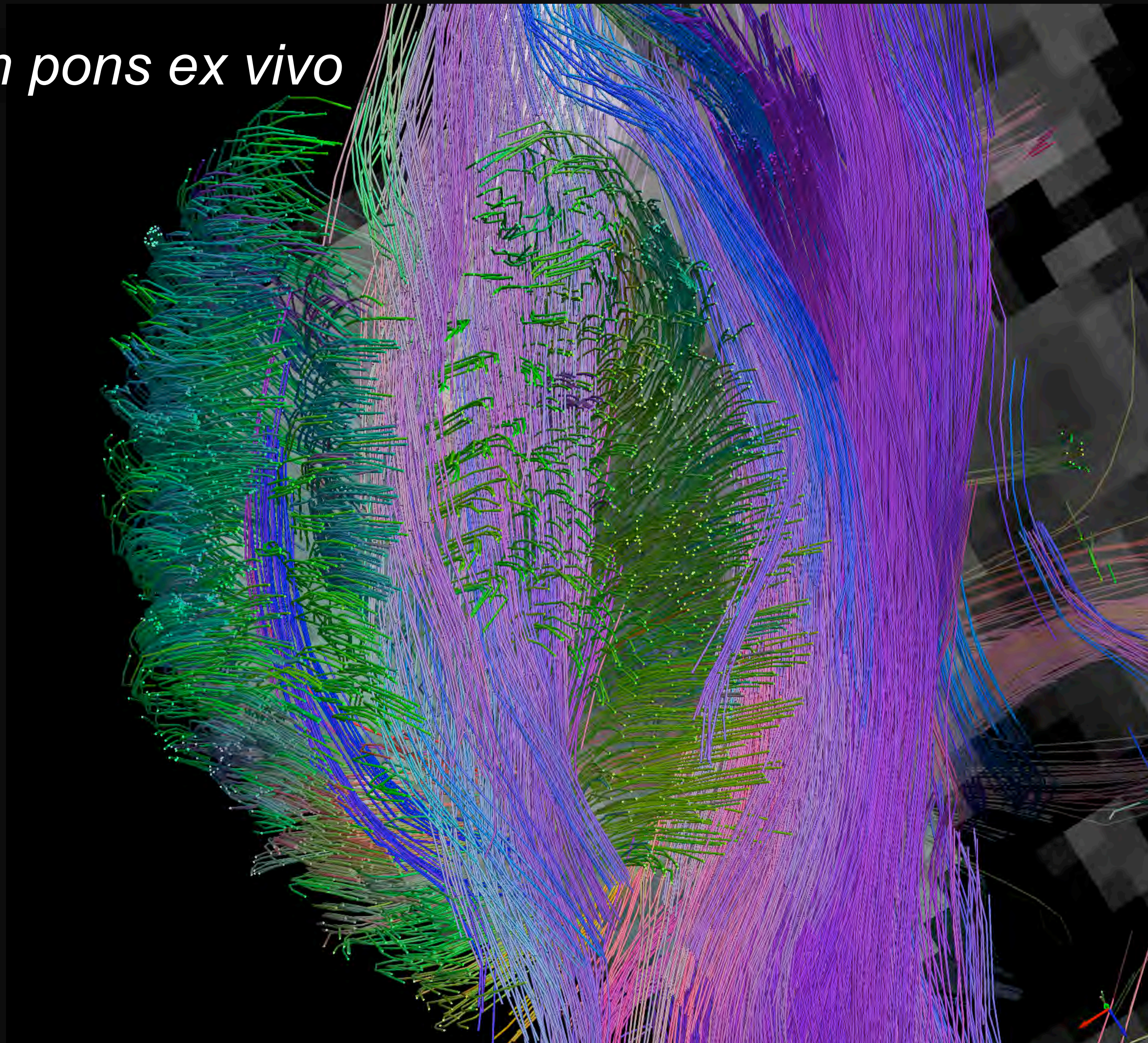

Esophagus fiber structure - like Chinese finger cuffs